Long-wavelength MHD stability at high pressure required for ITER and other next-step devices

- Motivation
  - The resistive wall mode (RWM) is a primary cause of plasma disruption at high β
  - Understanding passive stabilization physics determining RWM stability is critical to extrapolate stability requirements for future devices
  - Active control of RWM required when profile transients cause instability
- Passive stability: Very brief history
  - Early theory: RWM can be stabilized by sufficient plasma rotation
  - Critical ω_ϕ for passive stability assessed (Ω_{crit})
  - Low levels of Ω_{crit} (< 0.5% Alfven at q =2) suggested
  - RWMs found to be unstable at relatively high ω_ϕ, and stability depends on profile, not simple scalar value – no simple, low Ω_{crit}!
  - Stability model including kinetic effects evaluated (NSTX) - can explain greater complexity of experimental RWM marginal stability

Understanding plasma stability gradients vs. key profiles is essential for all operational states in devices such as ITER

- Current research focuses on:
  - greater understanding of the stabilization physics
  - projection to future devices
  - quantitative comparison to experiment
  - demonstration of improved active control techniques that can reduce resonant field amplification (RFA) or disruptions
- Outline
  - NSTX active feedback
    - Dual field component active control
    - Model-based state space controller
  - NSTX resonant field amplification experiments
    - Comparisons with kinetic theory: resonances and collisionality
  - ITER analysis with alpha particles and internal transport barriers

NSTX is a spherical torus equipped to study passive and active global MHD control, rotation variation by 3D fields

- High beta, low aspect ratio
  - R = 0.86 m, A > 1.27
  - I_p < 1.5 MA, B_t = 5.5 kG
  - β_t < 40%, β_N > 7
- Copper stabilizer plates for kink mode stabilization
- Midplane control coils
  - n = 1 – 3 field correction, magnetic braking of ω_ϕ by NTV
  - n = 1 RWM control
- Combined sensor sets now used for RWM feedback
  - 48 upper/lower B_p, B_r

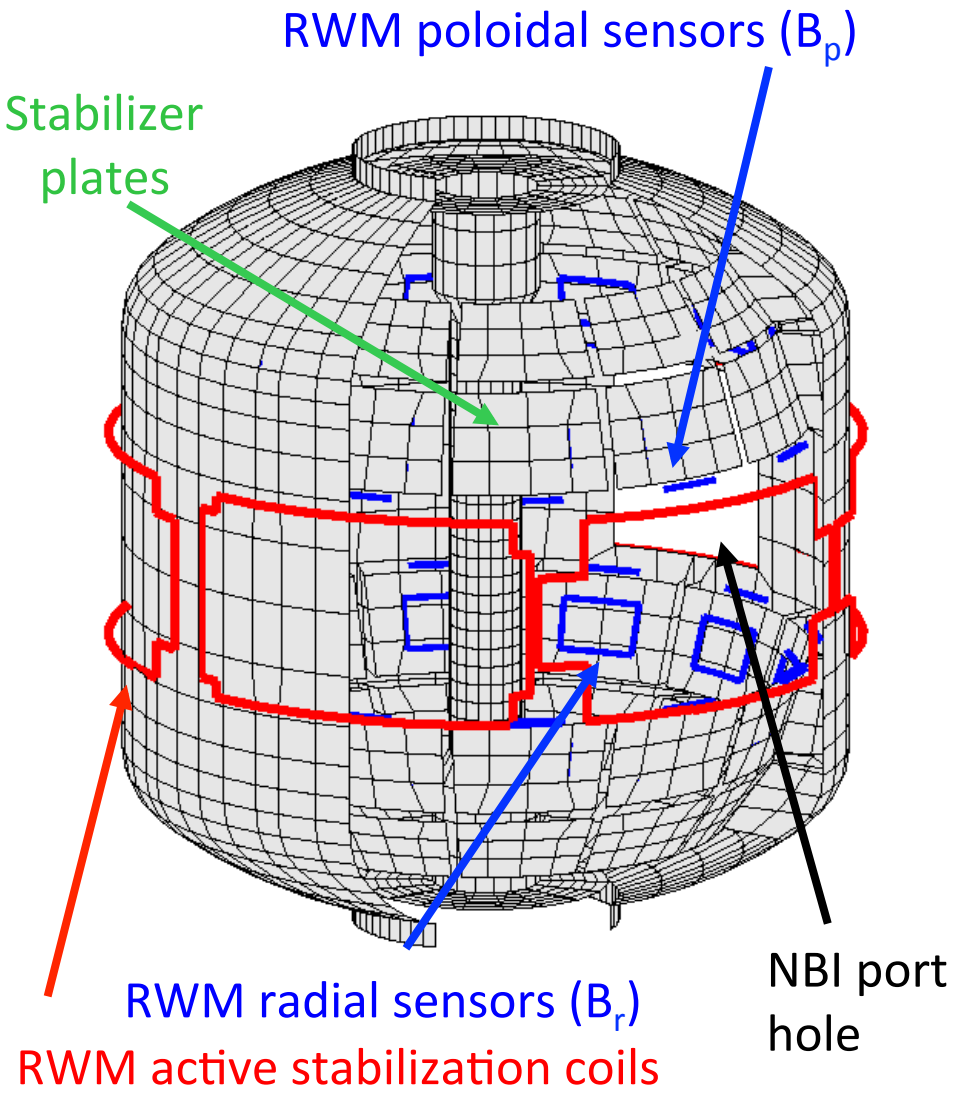

Kinetic terms in the RWM dispersion relation enable stabilization; theory consistent with experimental results

Dissipation (Im(δW_K)) and restoring force (Re(δW_K)) from kinetic term enables stabilization of the RWM:

$$(\gamma - i\omega_r)\,\tau_w = -\frac{\delta W_\infty + \delta W_K}{\delta W_b + \delta W_K}$$

[B. Hu *et al.*, Phys. Plasmas **12**, 057301 (2005)]

$$\delta W_K = \sum_j \sum_{l=-\infty}^{\infty} 2\sqrt{2}\pi^2 \int\int\int \left[|\langle H/\hat{\varepsilon}\rangle|^2 \frac{(\omega - n\omega_E)\frac{\partial f_j}{\partial \varepsilon} - \frac{n}{Z_j e}\frac{\partial f_j}{\partial \Psi}}{n\langle\omega_D^j\rangle + l\omega_b^j - i\nu_{\text{eff}}^j + n\omega_E - \omega} \right] \frac{\hat{\tau}}{m_j^{\frac{3}{2}} B} |\chi| \hat{\varepsilon}^{\frac{5}{2}} d\hat{\varepsilon} d\chi d\mathbf{\Psi}, \qquad \chi = v_\parallel / v$$

Precession Drift

Bounce

~ Plasma Rotation: $\omega_\phi \approx \omega_E + \omega_{*i}$

Collisionality

MISK Code

[γτ$_w$ contours vs. ν and ω$_\phi$]

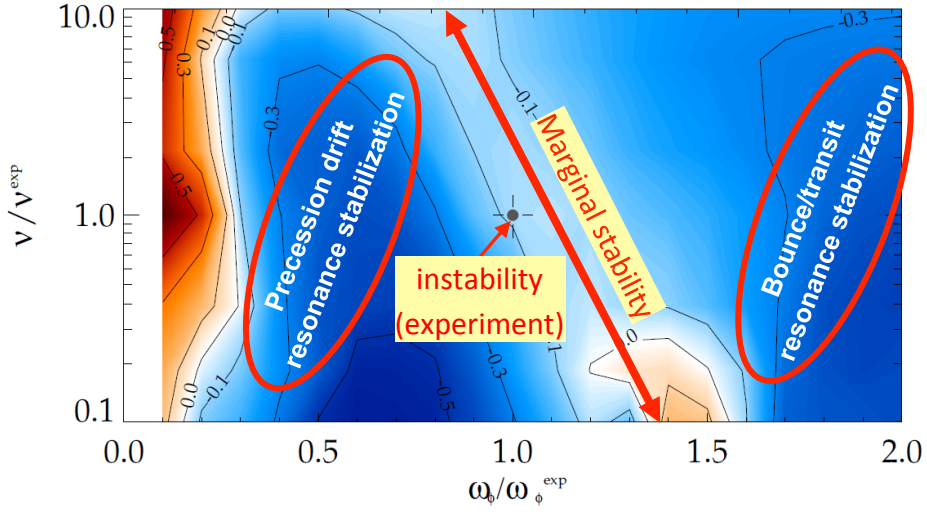

[S. Sabbagh *et al.*, IAEA 2010, EXS/5-5]

- MISK calculations are consistent with RWM instability at intermediate plasma rotation in NSTX
- Instability appears between precession drift resonance at low ω$_\phi$, bounce/transit resonance at high ω$_\phi$

[S. Sabbagh *et al.*, Nucl. Fusion **50**, 025020 (2010)]

[J. Berkery *et al.*, Phys. Rev. Lett. **104**, 035003 (2010)]

NSTX reaches high β_N, low l_i; RWM stability investigated in unstable plasmas, active control applied

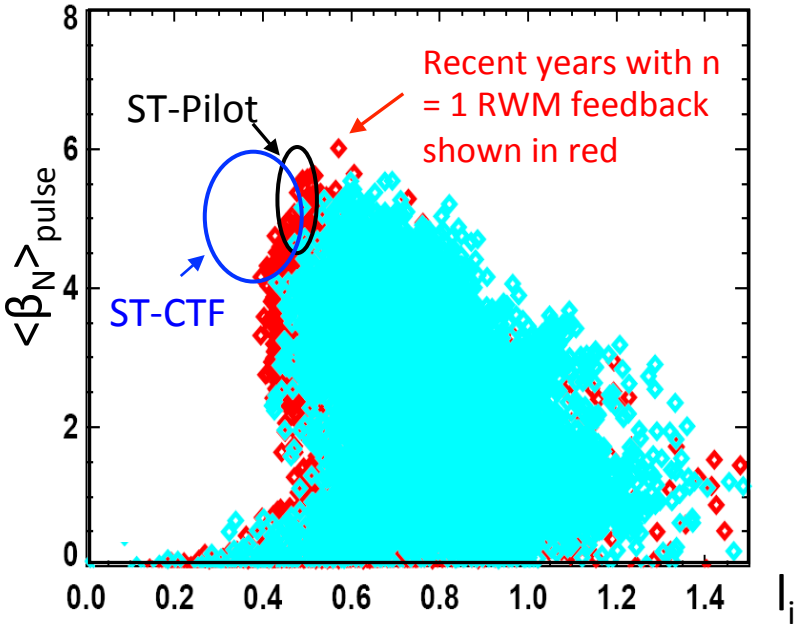

- NSTX plasmas have begun to reach low l_i and high $<\beta_N>_{pulse}$ suitable for next-step ST fusion devices
  - Some parameters (e.g. elongation > 3) still need to be reached self-consistently
  - Broad current profile → low l_i = $<B_p^2>/<B_p>_\psi^2$, has global mode stability implications

- Unstable plasma
  - Causes β collapse, I_p disruption
  - Correlate marginal stability point with kinetic theory MISK calculations

    or
  - Use active control to stabilize

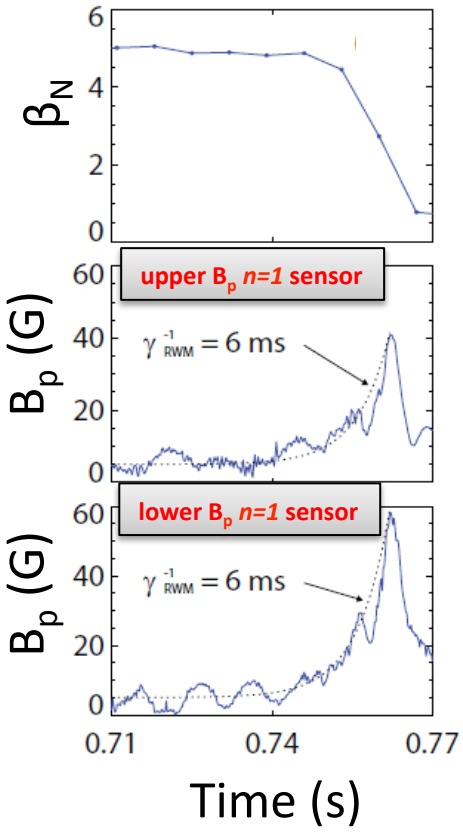

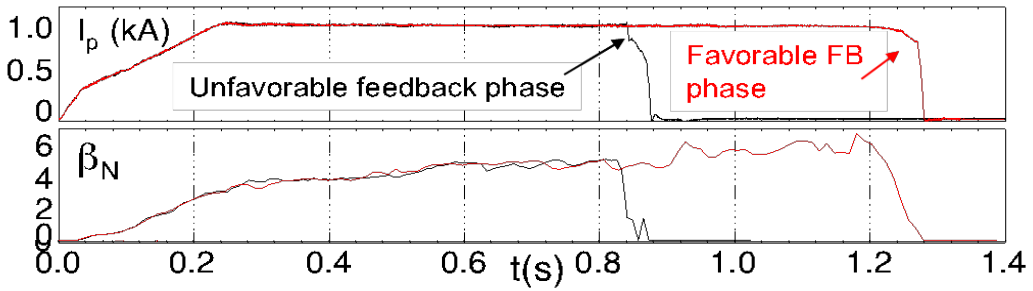

RWM B_r sensor n = 1 feedback phase variation shows superior settings when combined w/B_p sensors; good agreement w/theory so far

NSTX Experiments: B_p + B_r feedback

n = 1 B_r + B_p feedback
(B_p gain = 1, B_r gain = 1.5)

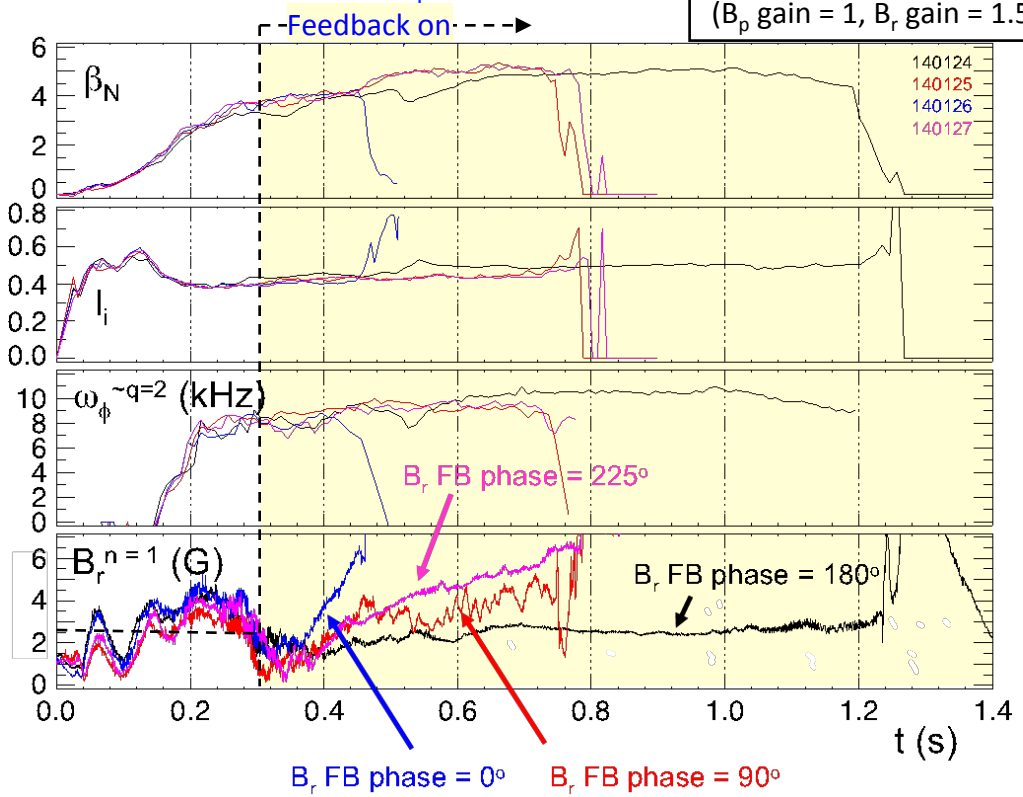

VALEN calculation of NSTX B_r + B_p control

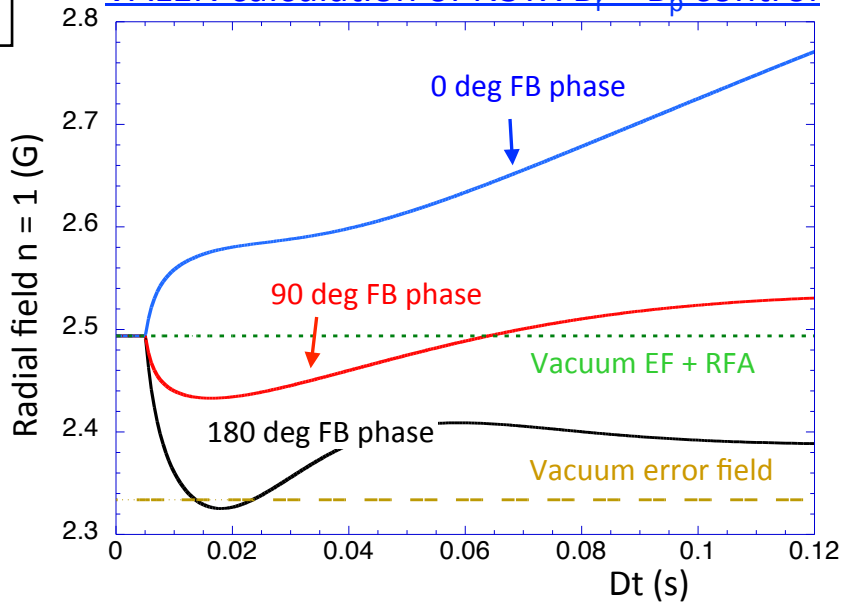

- Favorable (experimental) B_p feedback settings, varied B_r settings
  - Positive/negative feedback produced at theoretically expected phase values

- VALEN calculation of B_r+B_p feedback follows experiment
  - stable plasma (negative "s")
  - Now examining plasma response model variation
    - impact of "s", and diff. rotation ("α") on results

RWM feedback using upper/lower B_p and B_r sensors shows good agreement with B_r feedback phase; gain not optimized

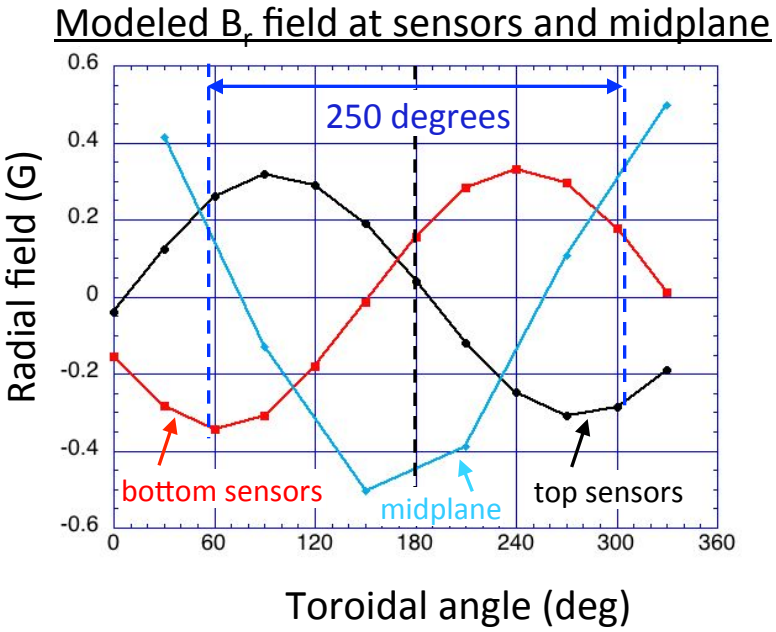

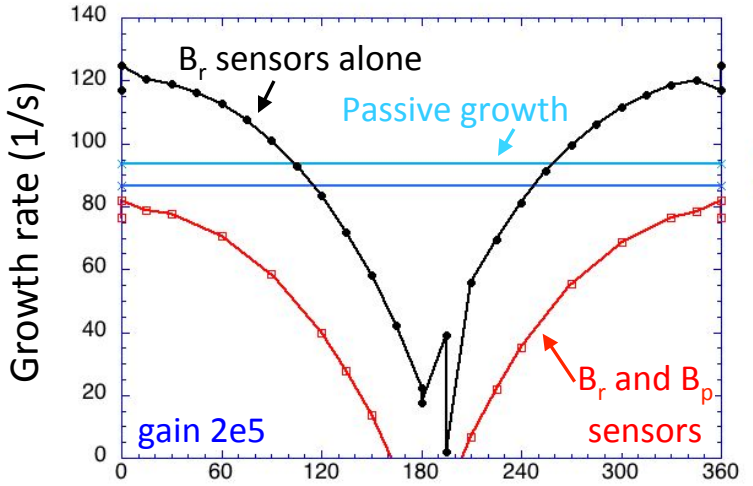

DCON, VALEN codes

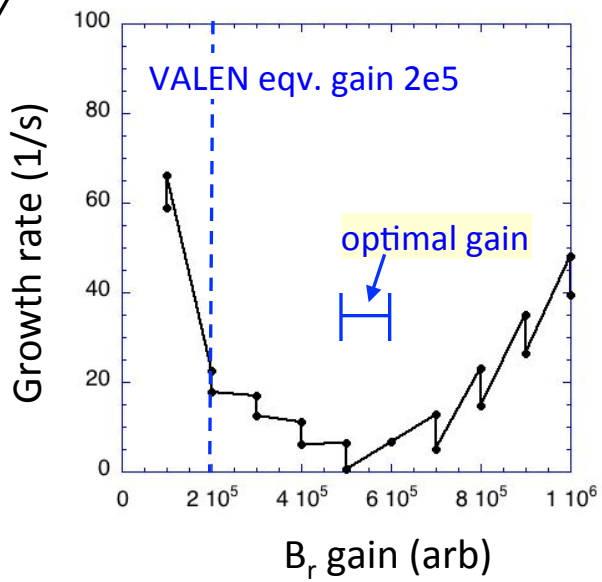

- Both B_r, B_p feedback contribute to active control
  - B_r mode structure and optimal feedback phase agrees with parameters used in experiment
  - B_r feedback alone provides stabilization for growth times down to ~ 10 ms with optimal gain
  - Physics of best feedback phase for B_p sensors in low l_i plasmas under investigation

New RWM state space controller implemented to best sustain high β_N

Full 3-D model

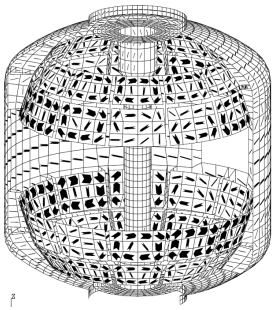

~3000+ states

Balancing transformation

State reduction (< 20 states)

RWM eigenfunction (2 phases, 2 states)

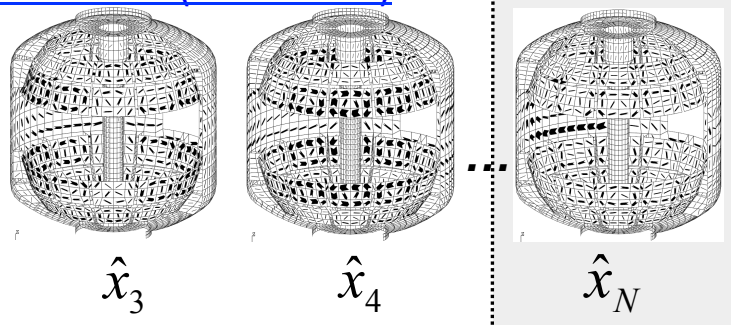

Controller reproduction of applied n = 1 field

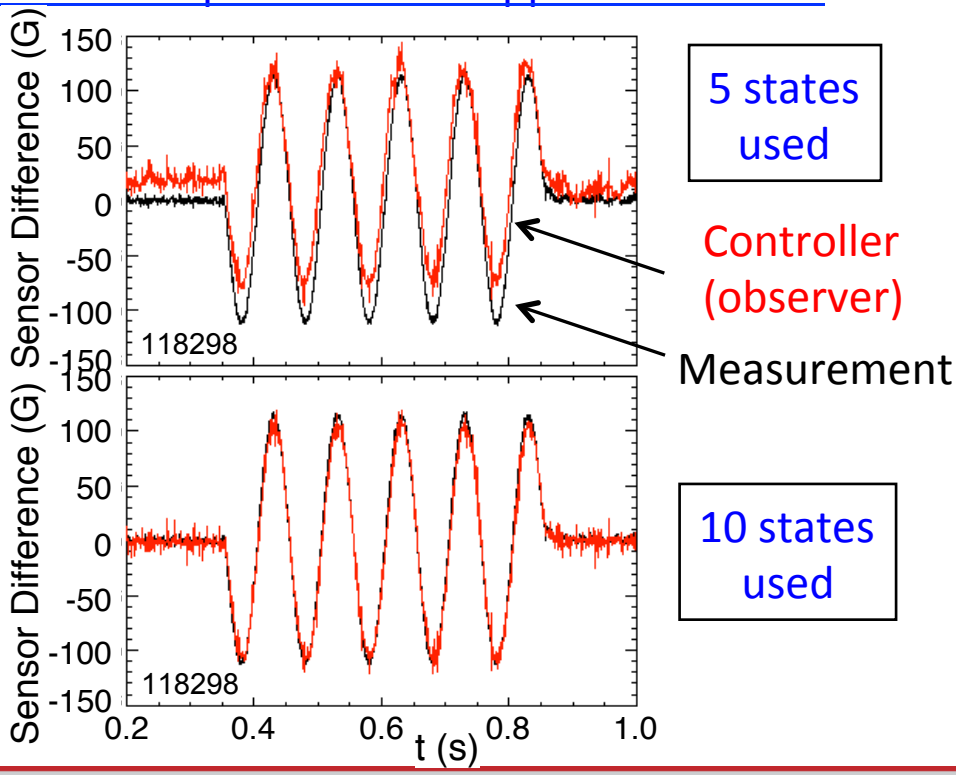

- Controller models, can compensate for wall currents
  - Including mode-induced current
- Potential to allow more flexible control coil positioning
  - May allow control coils to be moved further from plasma, and be shielded (e.g. for ITER)

[O. Katsuro-Hopkins *et al.*, Nucl. Fusion **47**, 1157 (2007)]

- Straightforward inclusion of multiple modes (n > 1) in feedback

Increased number of states in RWM state space controller improves match to sensors over entire mode evolution

RWM Upper B_p Sensor Differences (G) – 2 States

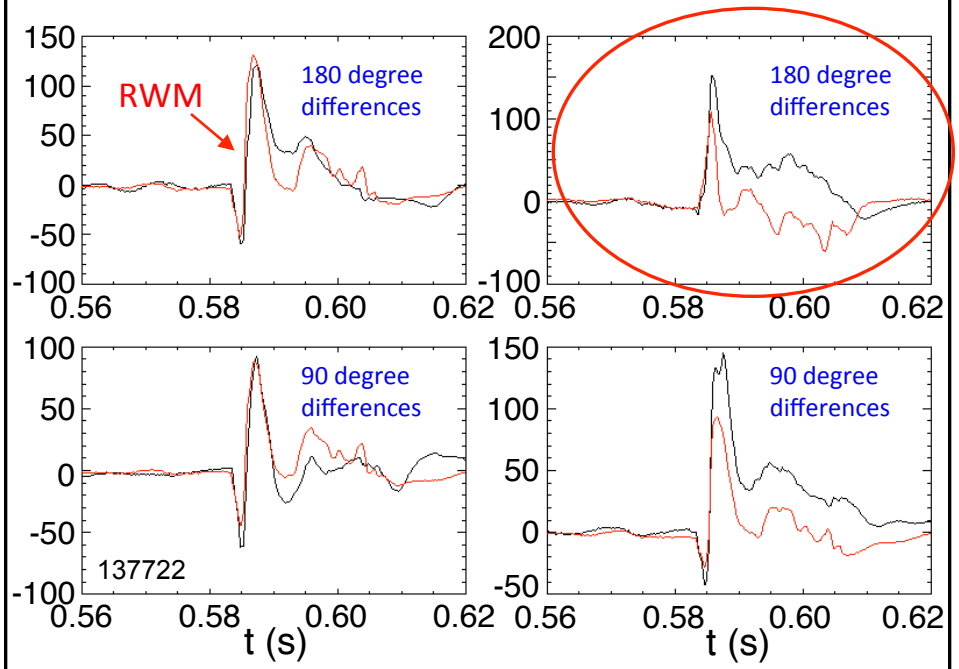

- Reasonable match to all B_p sensors during RWM onset, large differences later in evolution

RWM Upper B_p Sensor Differences (G) – 7 States

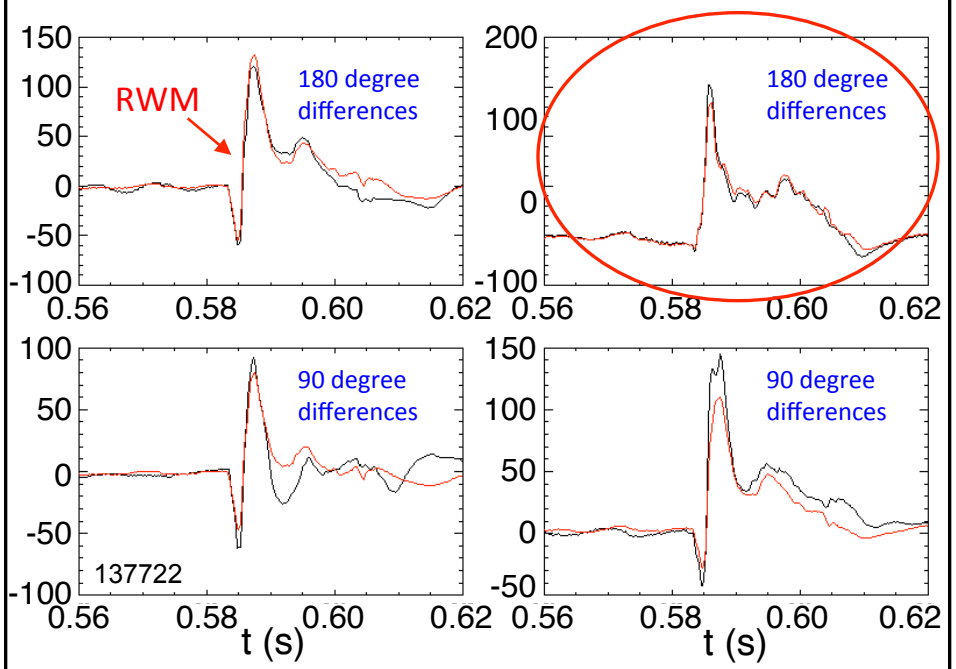

- Some 90 degree differences not as well matched
  - May indicate the need for an n = 2 eigenfunction state

Black: experiment Red: offline RWM state space controller

3-D conducting structure detail can improve RWM state space controller match to sensors

RWM Lower B_p Sensor Differences (G) – NO PORT

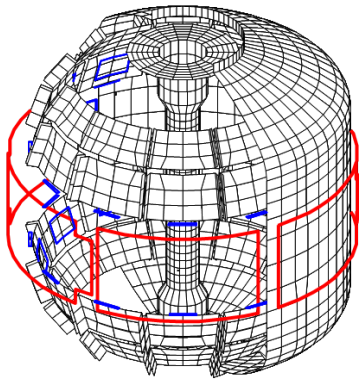

- Some 90 degree differences not well matched

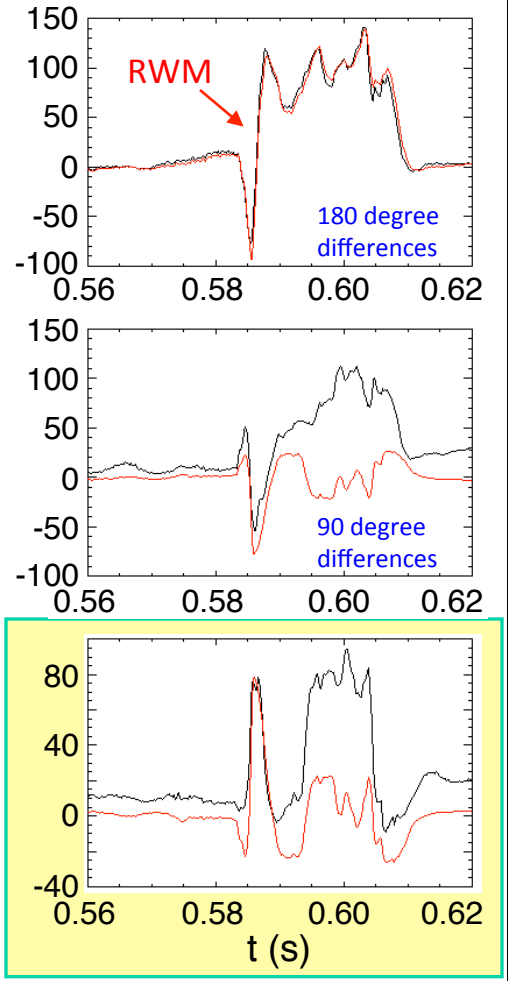

RWM Lower B_p Sensor Differences (G) – NBI PORT

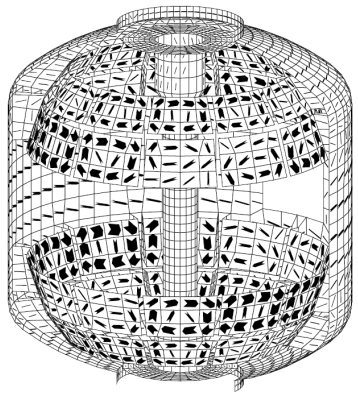

- Adding NBI port leads to greater match on some sensors

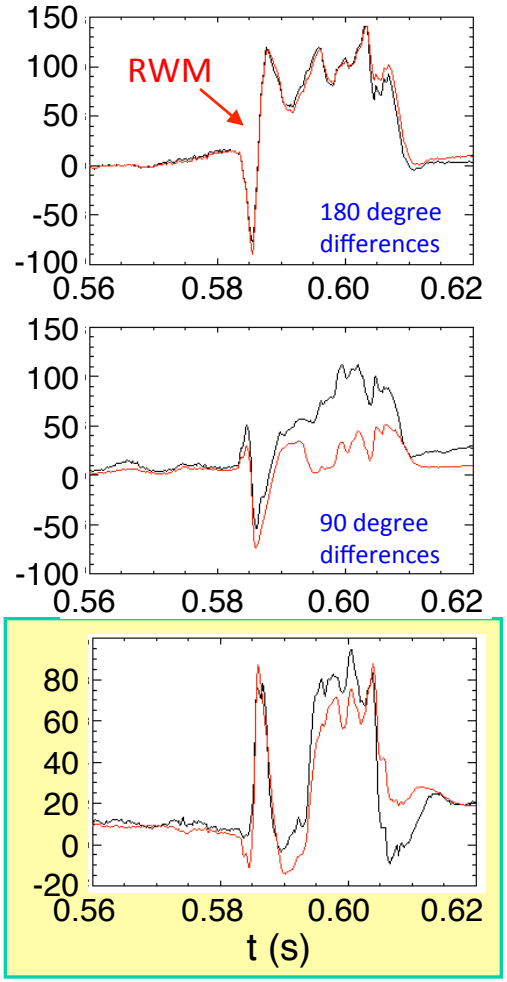

Black: experiment Red: offline RWM state space controller

New RWM state space controller sustains high β_N, low l_i plasma

- RWM state space (12 states) feedback phase scan
  - Best feedback phase produced long pulse, $\beta_N = 6.4$, $\beta_N/l_i = 13$

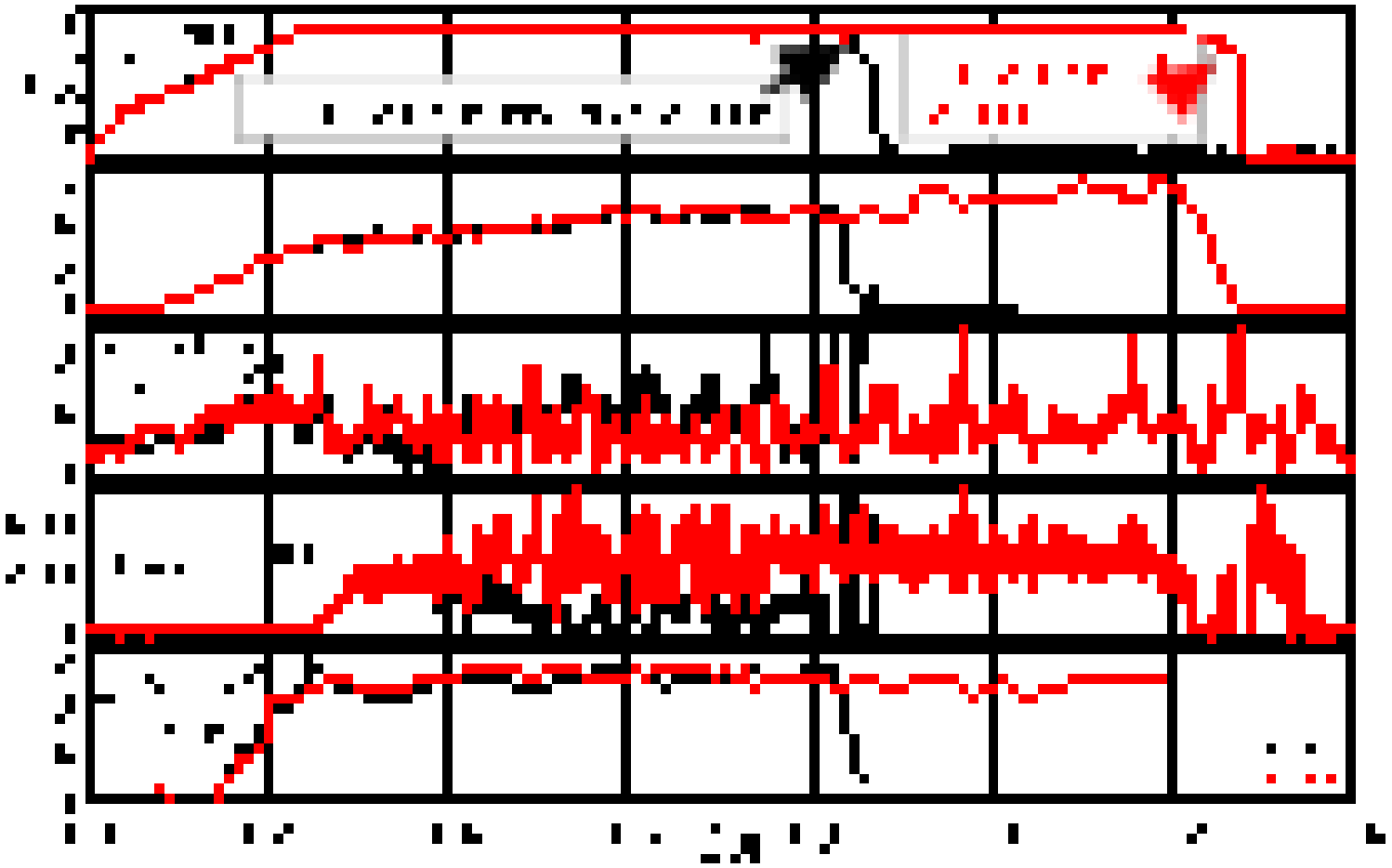

RWM state space controller sustains otherwise disrupted plasma caused by DC n = 1 applied field

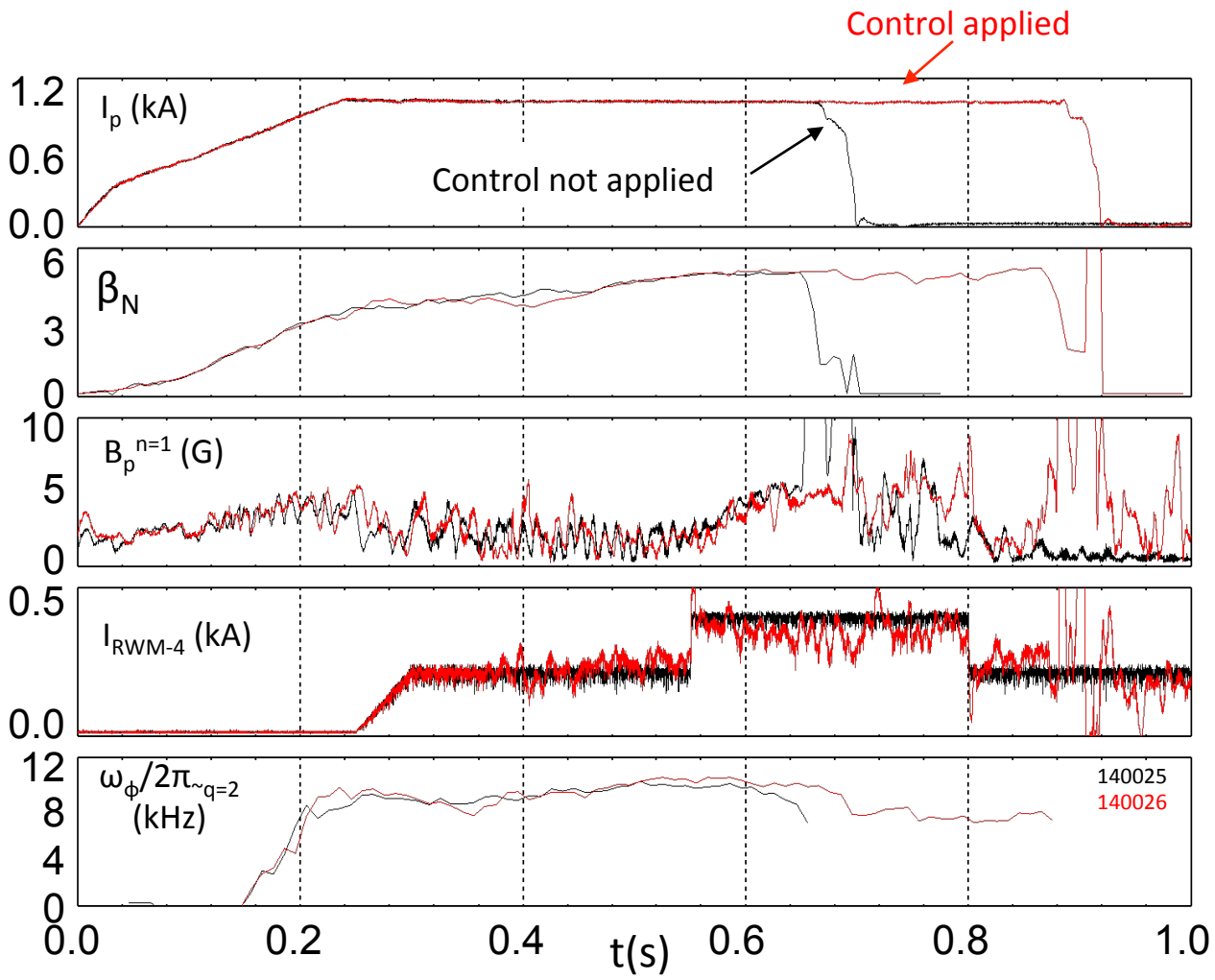

- n = 1 DC applied field
  - Simple method to generate resonant field amplication
  - Can lead to mode onset, disruption
- RWM state space controller sustains discharge
  - With control, plasma survives n = 1 pulse
  - n = 1 DC field reduced
  - Transients controlled and do not lead to disruption
  - NOTE: initial run – gains NOT optimized

Active MHD spectroscopy is used to probe plasma stability

- Active MHD spectroscopy used as a proxy for RWM stability when modes are stable
  - Resonant field amplification (RFA) of an n=1 applied AC field is measured.
  - Increased RFA indicates decreased stability

$$RFA = \frac{B_{plasma}}{B_{applied}}$$

[H. Reimerdes *et al.*, Phys. Rev. Lett. **93**, 135002 (2004)]

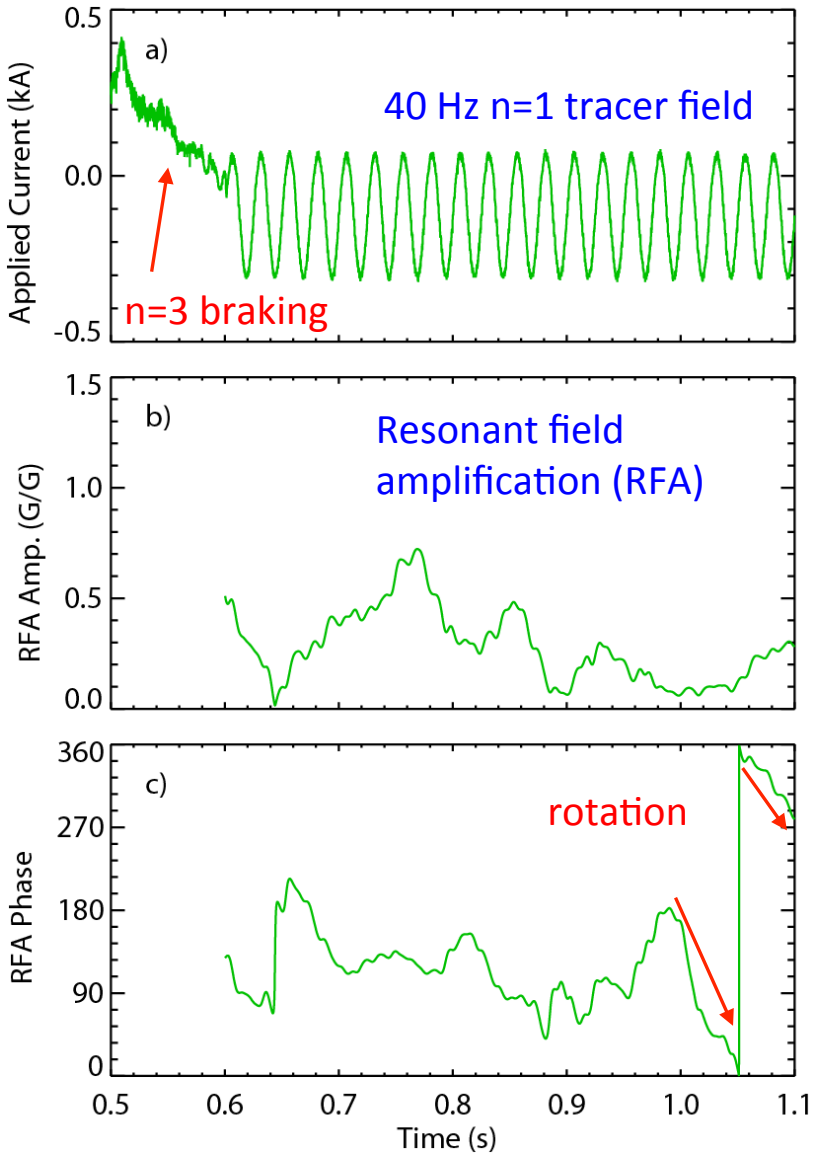

Resonant field amplification experiments in NSTX gauge the stability of plasmas to compare to kinetic stabilty theory

- Experiments in NSTX measured RFA of high beta plasmas with rotation slowed by n=3 magnetic braking.
  - 140094: unstable at 0.9 s
  - 140092: same β, higher rotation: remains stable (though approaches marginal twice)
  - 133776: higher β, same rotation: marginally stable
  - 140102: higher β, lower rotation, but stable! Counter-intuitive without invoking kinetic effects

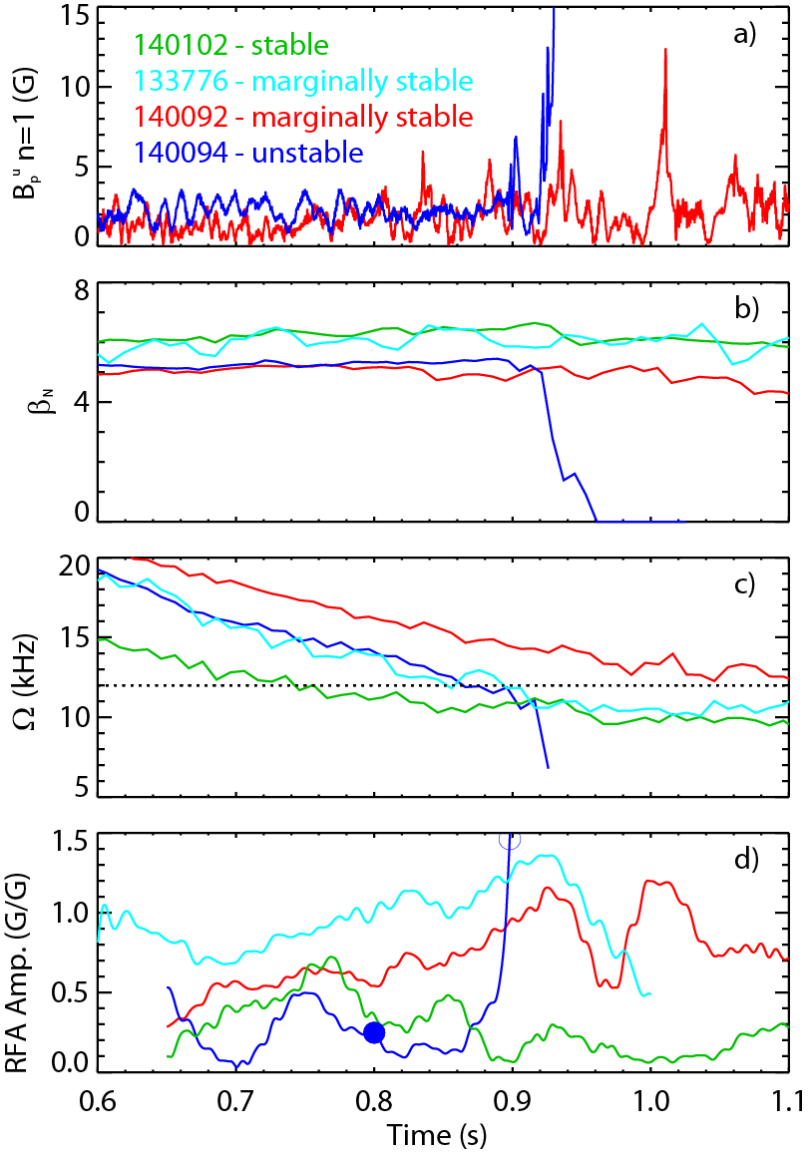

RFA measurements add additional support to established theory of RWM stability through kinetic resonances

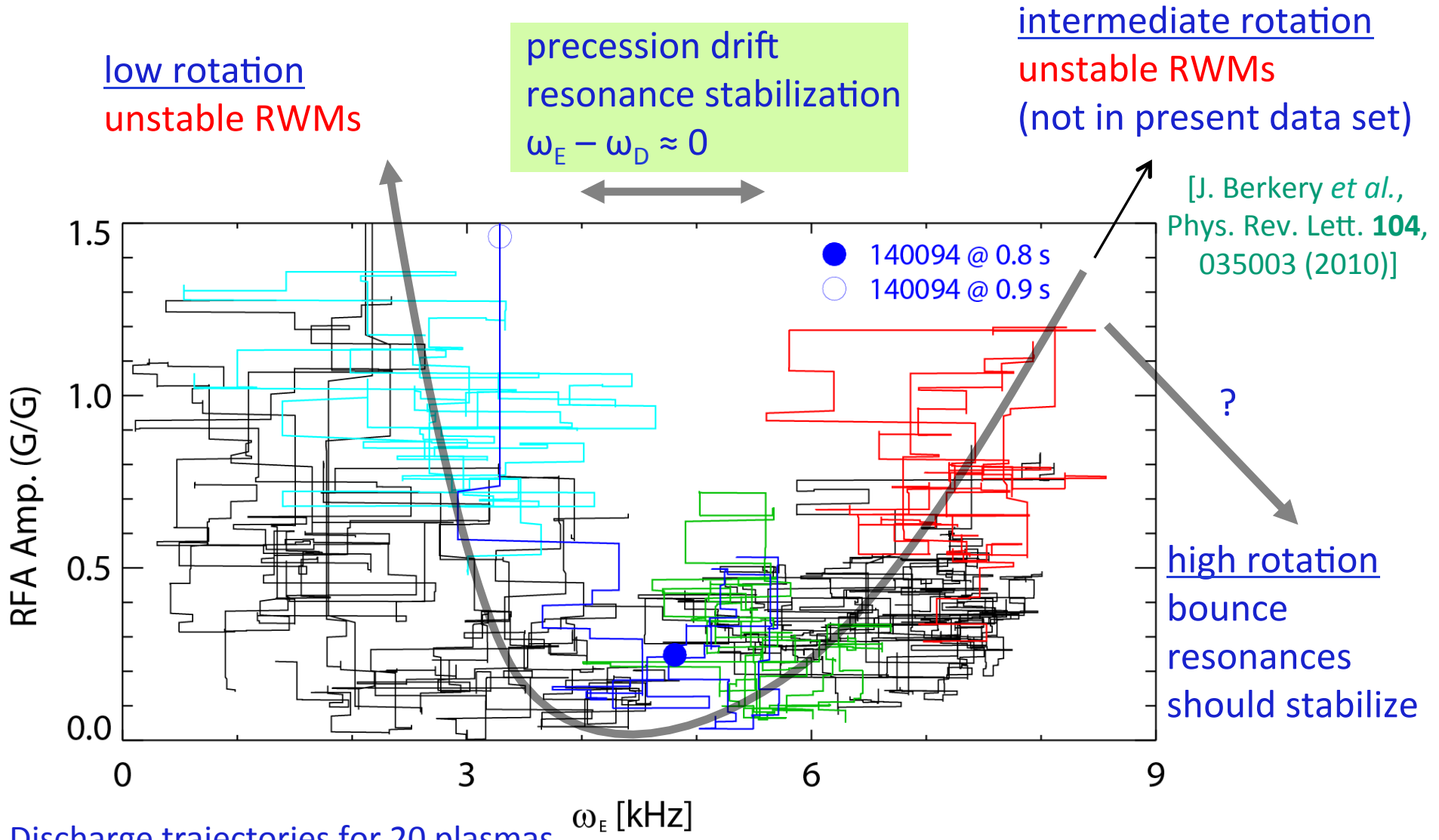

Discharge trajectories for 20 plasmas

Experimental instability can be explained by kinetic theory and MISK calculation

- Earlier time (0.8 s, ●):
  $\omega_E \approx \omega_D$
  - Experiment: stable
  - Theory: stabilizing
  - Calculation: stable
- Later time (0.9 s, ○):
  $\omega_E < \omega_D$
  - Experiment: unstable
  - Theory: destabilizing
  - Calculation: unstable (at 10% lower rotation)

Experiment (RFA)

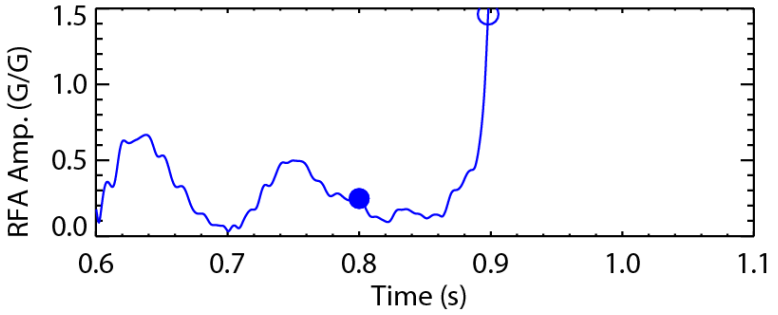

Profiles (Theory)

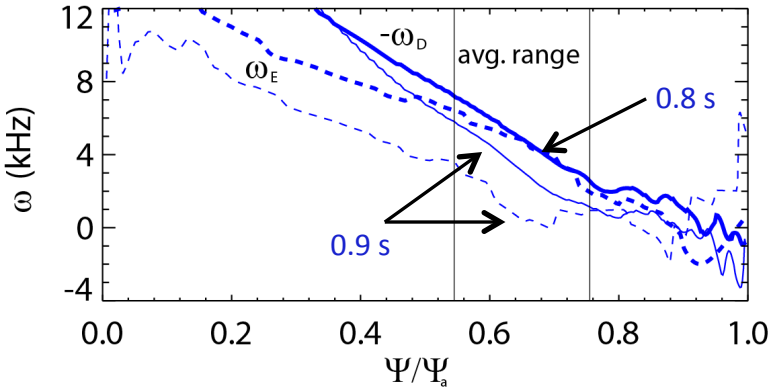

MISK Calculation

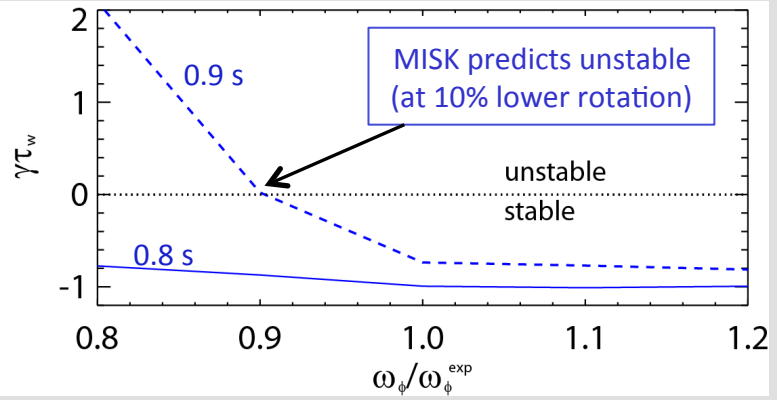

Notes: ω_D shown is for zero pitch angle and ε/T = 2.5 (higher than usual). MISK calculation doesn't include EPs

RFA measurements confirm previous NSTX result that the highest β_N/l_i is not the least stable

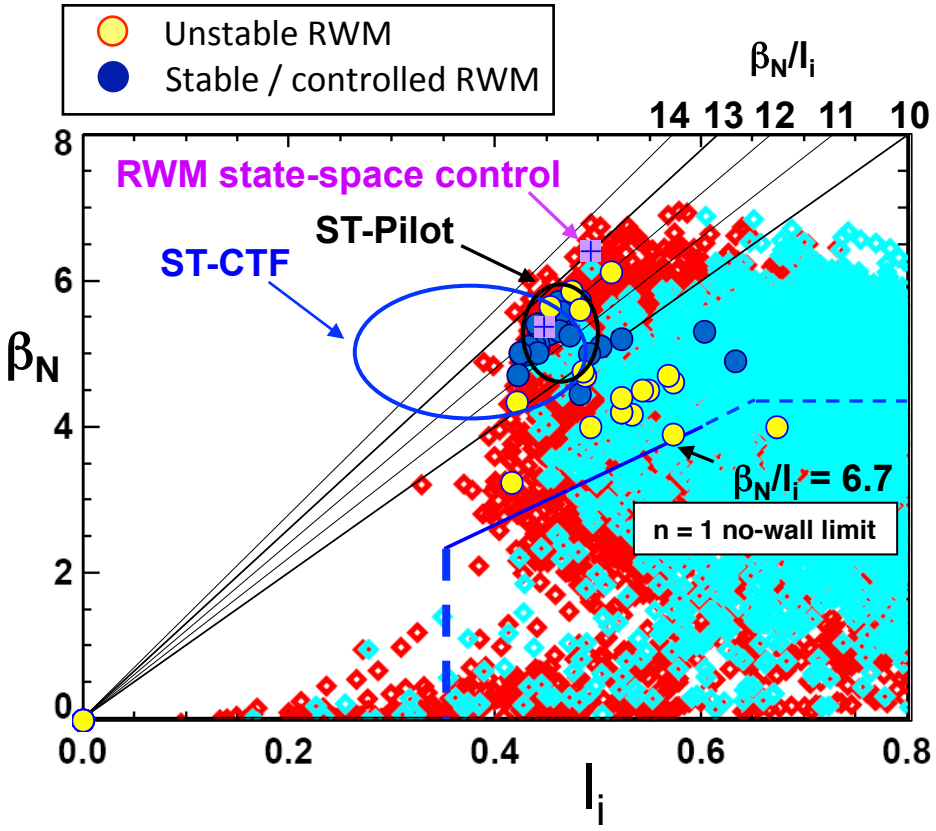

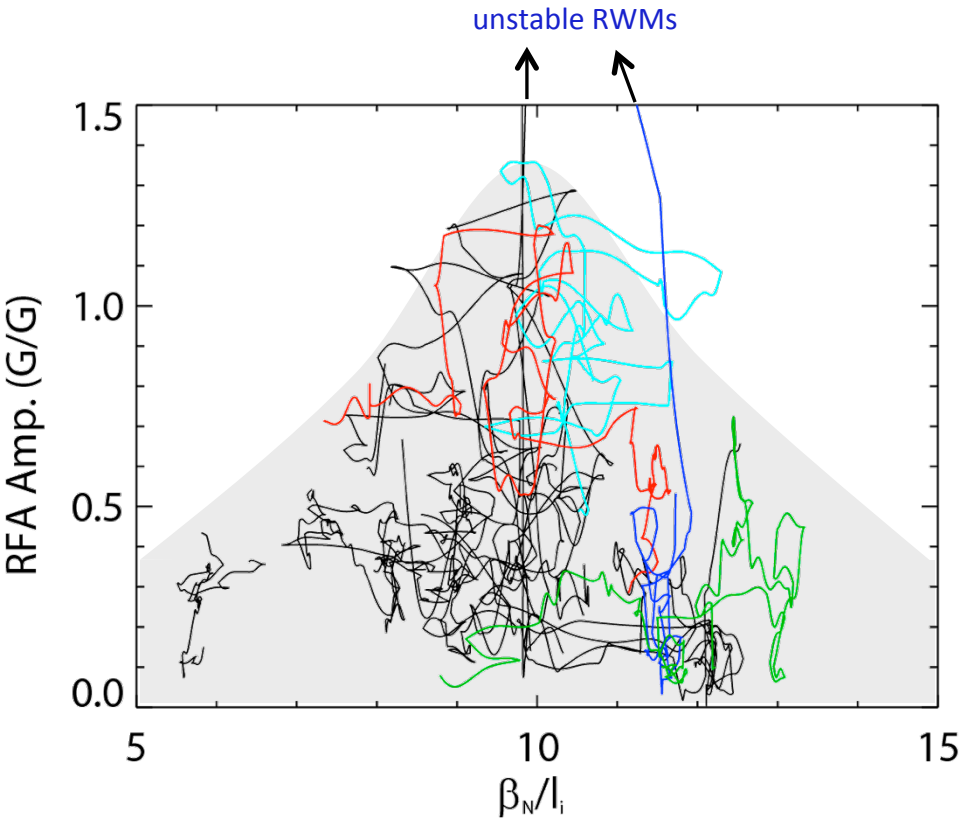

- NSTX can reach high β, low l_i range where next-step STs aim to operate
  - Active control experiments reduced disruption probability from 48% to 14%, but mostly in high β_N/l_i
- RFA amplitude from 20-shot database also peaks at intermediate β_N/l_i
  - Increased stability at high β_N/l_i due to kinetic stabilization from resonances

Theory: Reduced ν is stabilizing near kinetic resonances Experimental Confirmation: Reduced ν -> reduced low RFA

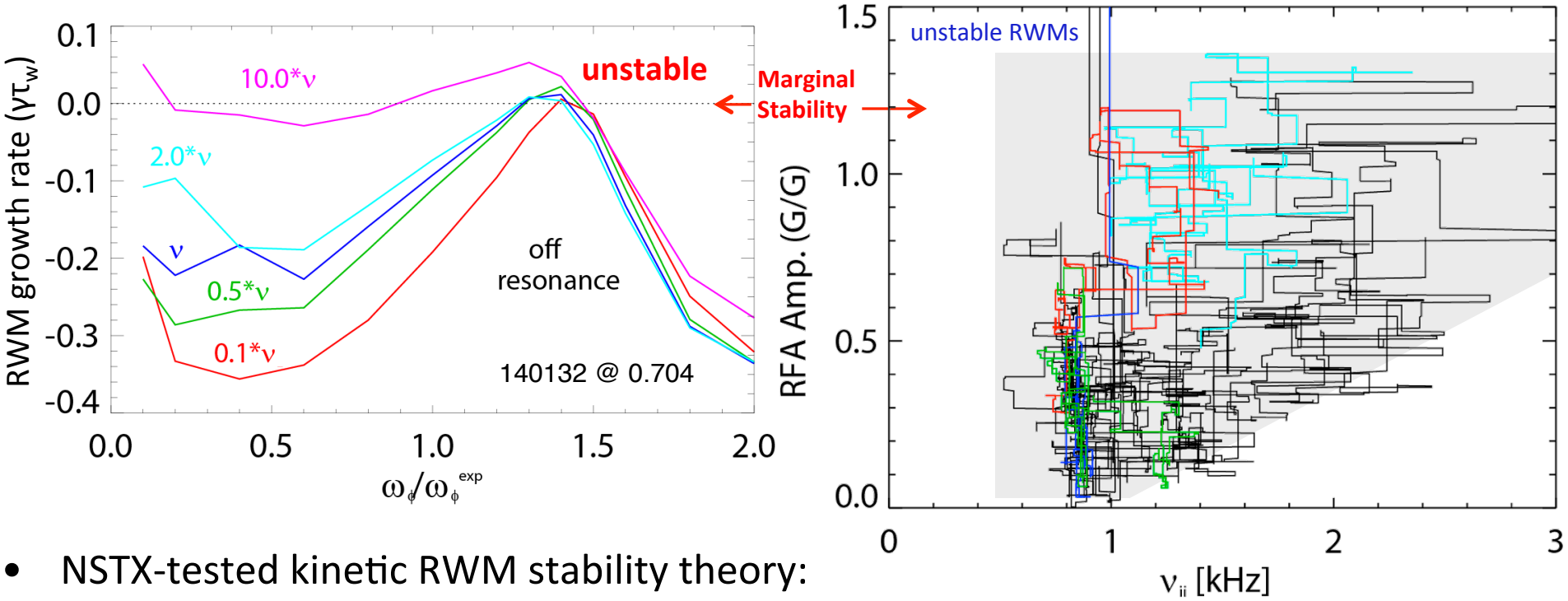

- NSTX-tested kinetic RWM stability theory:
  - Stabilizing collisional dissipation reduced (expected from early theory)
  - Stabilizing resonant kinetic effects enhanced (contrasts early RWM theory)
- RFA amplitude reduced at lower ν for low RFA (stable) plasmas, little effect on higher RFA (marginal) plasmas
- Expectations in NSTX-U, tokamaks at lower ν (ITER)
  - Stronger stabilization near ω_ϕ resonances; almost no effect off-resonance

[J. Berkery *et al.*, Phys. Rev. Lett. **106**, 075004 (2011)]

Agreement achieved between MISK and MARS-K under ITPA MHD Stability Group MDC-2 Benchmarking

Work in progress!

	r_{wall}/a	Ideal $\delta W/-\delta W_\infty$	$Re(\delta W_k)/\delta W_\infty$	$Im(\delta W_k)/(\delta W_\infty)$	$\gamma\tau_{wall}$	$\omega\tau_{wall}$	$\delta W_k/-\delta W_\infty$ ($\omega_E = \infty$)
Solov'ev 1	1.15						
(MARS-K)		1.187	0.0256	-0.0121	0.804	-0.0180	0.157
(MISK)		1.122	0.0271	-0.0077	0.847	-0.0124	0.153
Solov'ev 3	1.10						
(MARS-K)		1.830	0.209	-0.342	0.350	-0.228	4.51
(MISK)		2.337	0.219	-0.128	0.302	-0.065	0.898
ITER	1.50						
(MARS-K)		0.682	-4.51	-0.445	-1.43	-0.050	229
(MISK)		0.677	0.653	-0.746	-0.041	-0.538	8.46

- Calculations from MISK, and MARS-K (perturbative)
  - The relevant frequencies and eigenfunctions now match between codes for both analytical Solov'ev and ITER equilibria.
  - Numerical approach to the frequency resonance fraction energy integral taken in MISK is equivalent to analytical limits computed in MARS-K.

Agreement achieved between MISK and MARS-K under ITPA MHD Stability Group MDC-2 Benchmarking

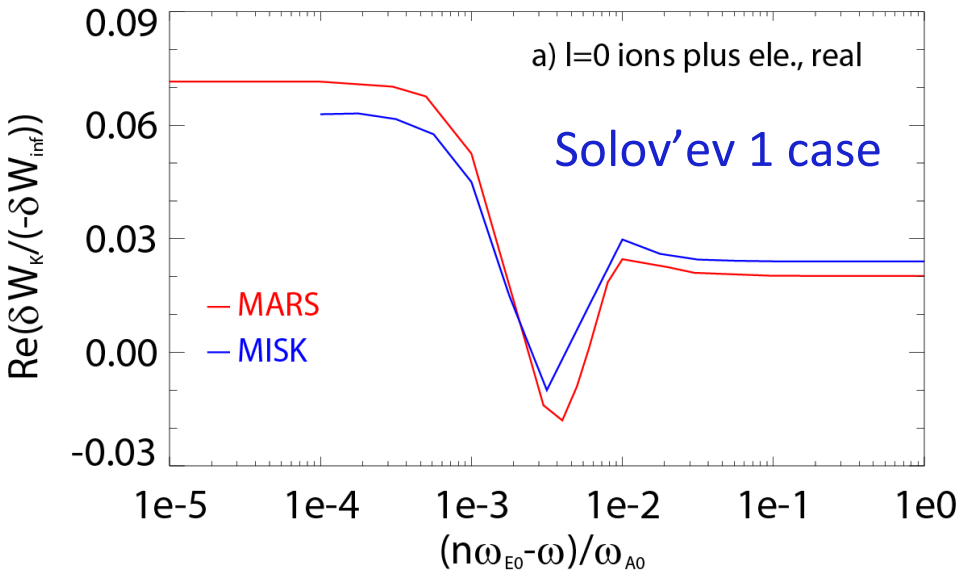

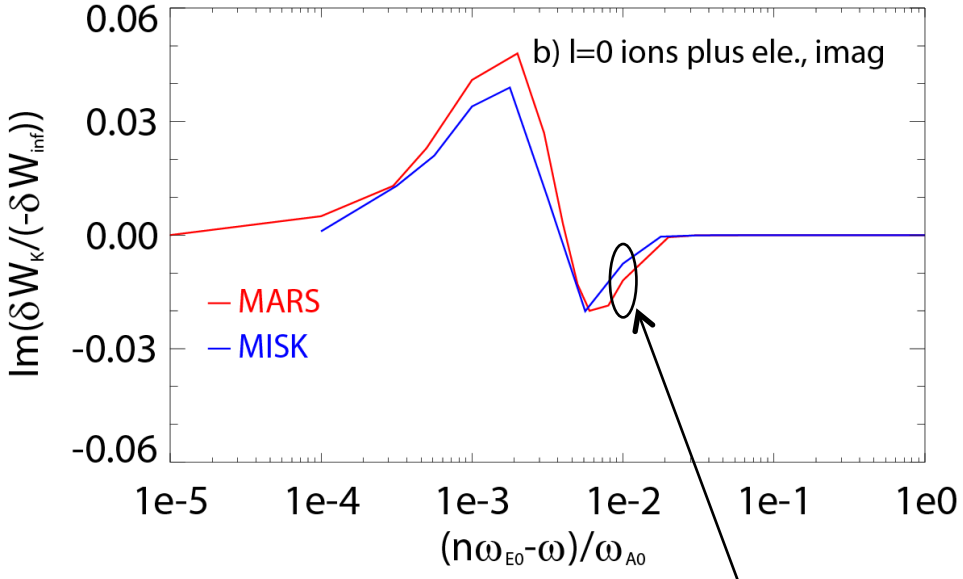

- Comparing δW_K vs. ω_E scan (rather than single point (ω_E = 1e-2) in chart)
  - Good agreement for precession drift resonance (l=0 trapped particles) and circulating particles
  - "Light green" in chart can be deceiving: really OK agreement

$Im(\delta W_k)/(\delta W_\infty)$
-0.0121
-0.0077

ITER advanced scenario requires alpha particles for RWM stability across all rotation values

In a previously analyzed case [J.W. Berkery *et al.*, Phys. Plasmas 17, 082504 (2010)], αs were required for stability across all ω_ϕ.

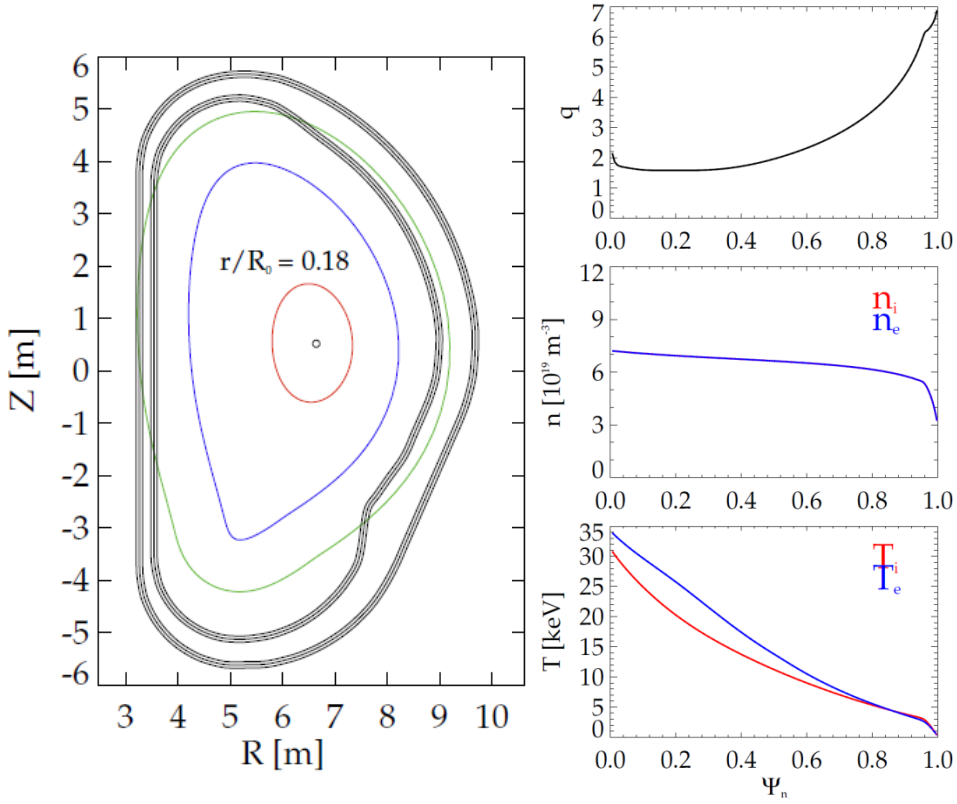

- ITPA MHD WG7 equilibrium
  - I_p = 9 MA, β_N = 2.9 (7% above no-wall limit)

$\gamma\tau_w$ contours vs. β_α and ω_ϕ

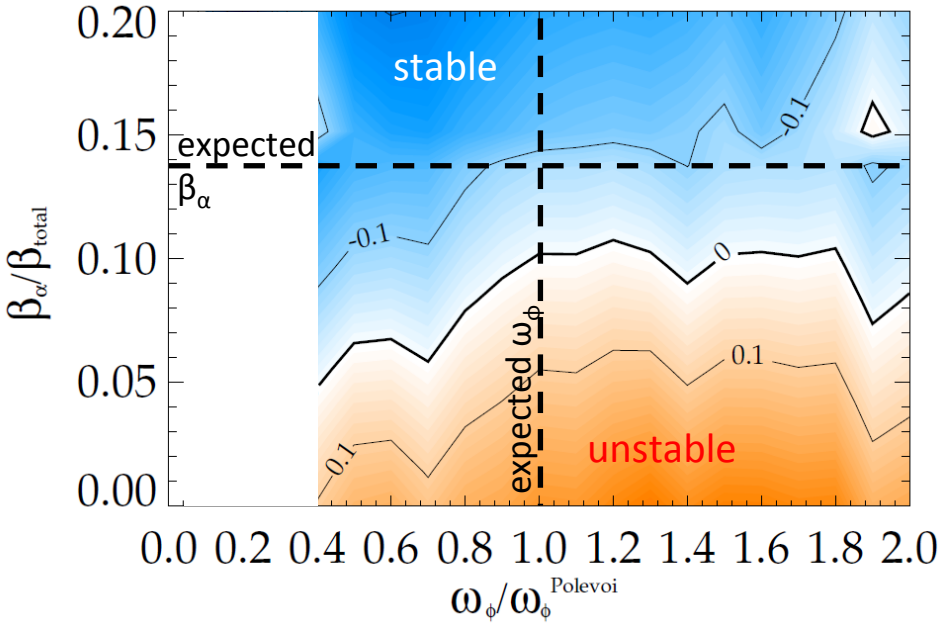

- Calculation revisited with physics improvements (inc. correction to ω_D in MISK)
  - Makes calculation somewhat more stable, but generally consistent. Doesn't affect the conclusions.

Kinetic RWM stability analysis started with MISK for a wider database of ITER advanced scenario equilibria

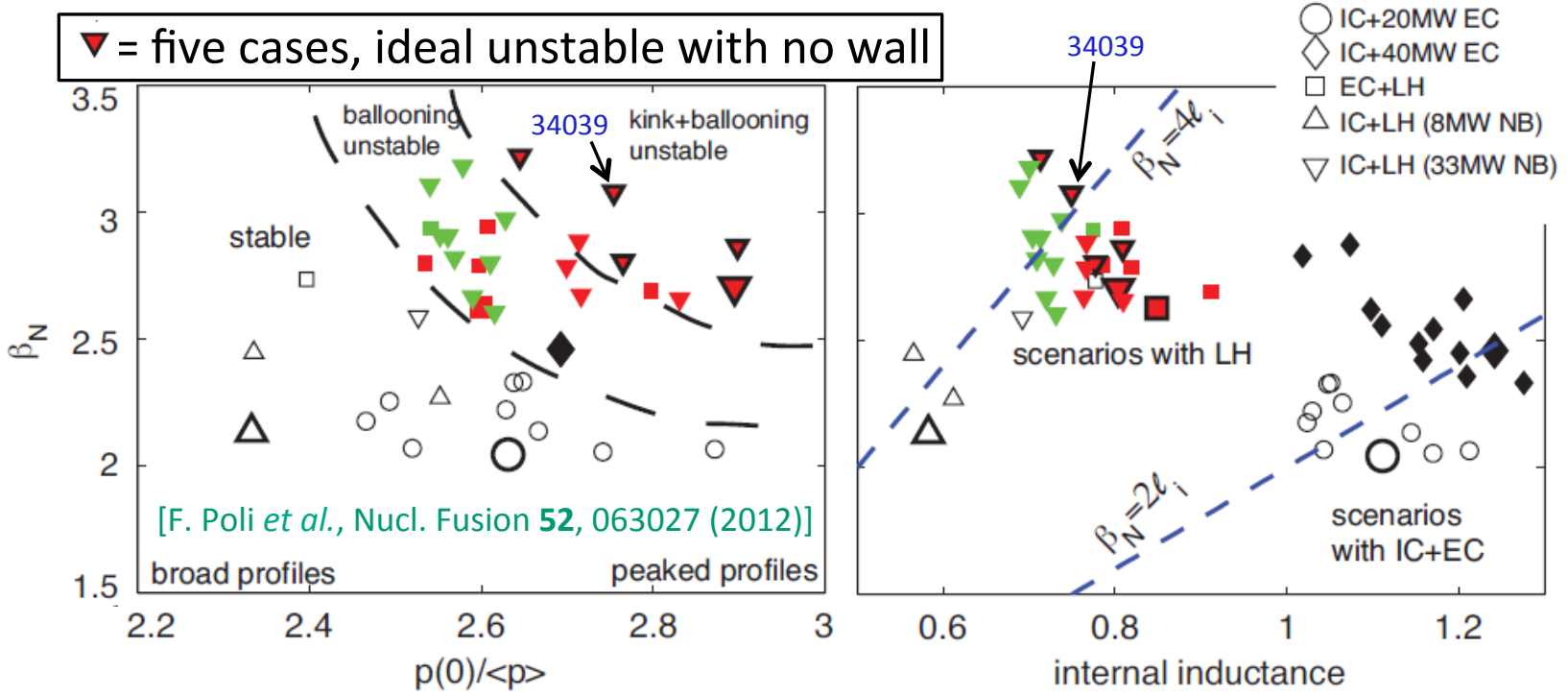

- Five discharges selected; self-consistent variation in parameter space
  - Full discharge evolutions – created by combination of TSC and TRANSP codes
  - Range of β_N = 2.65 – 3.25; ideal n=1 no-wall unstable
  - Have internal transport barriers
- Include EPs from: 33MW N-NBI (D), 20 MW IC, 40 MW LH
  - Next steps: include anisotropic EP dist.: slowing-down for beams, bi-Max for RF.

Low rotation, ITBs in ITER can cause stabilizing precession drift resonance in plasma core

- "Infernal" type eigenfunction peaks near core.
- Strong internal gradients create large ω_*
  - Cause difference between ω_ϕ and ω_{EXB}.
  - Enables resonance with precession drift of trapped thermal ions if ω_ϕ is low.

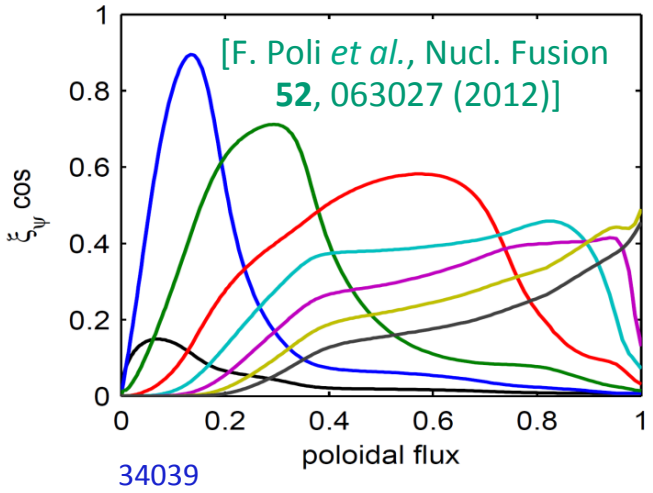

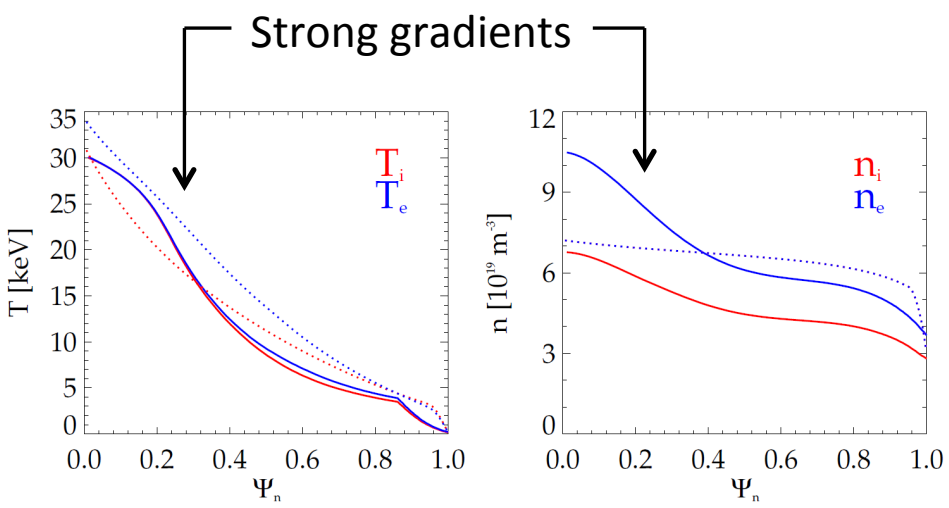

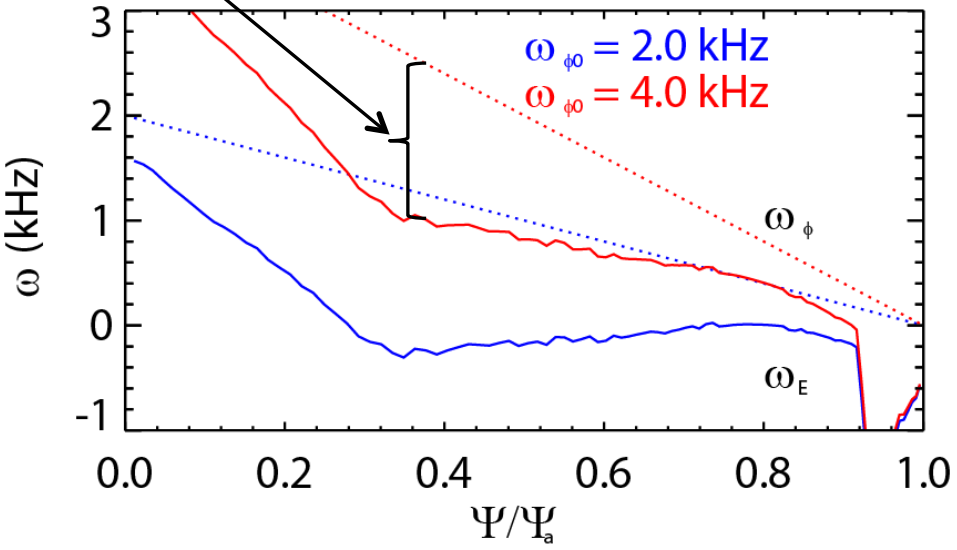

dashed lines = "standard" ITER advanced scenario

$$\omega_\phi \approx \omega_E + \omega_{*i}$$

Internal transport barriers may be beneficial to RWM stability by lowering the E×B frequency

- Stable region found with no alphas
  - At low ω_ϕ, due to precession resonance of trapped thermal ions, coupled with infernal eigenfunction
  - Unstable region at higher ω_ϕ similar to previous results

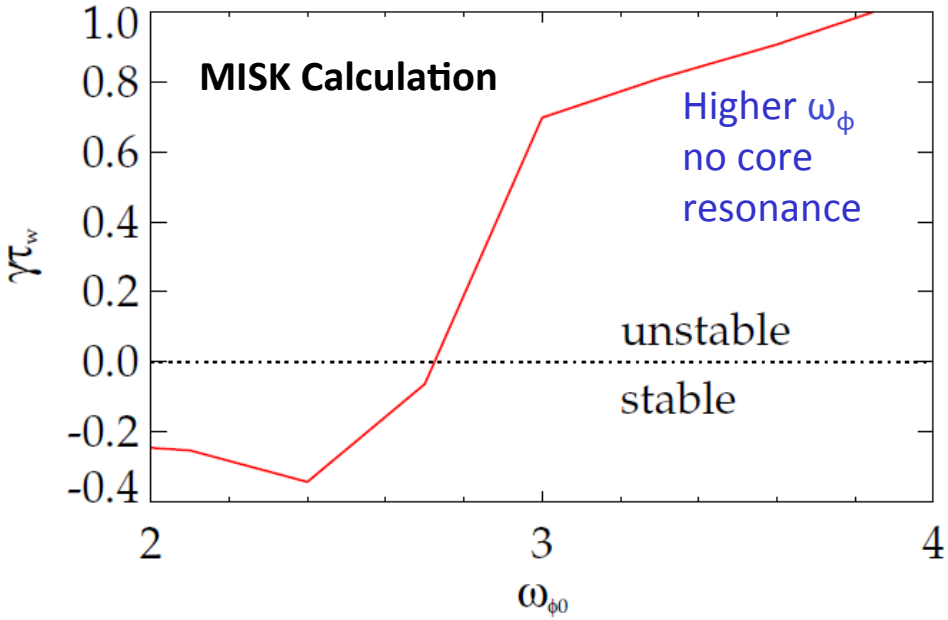

- Caveat: ITBs can be transient
  - This may result in RWM instability if profile dynamics move the plasma off-resonance
  - Active RWM control would then be needed during the period when the plasma profiles are away from stabilizing kinetic resonances

Global mode control and stabilization studies in high-β NSTX plasmas aid the goal of disruption avoidance in ITER

- Two active control techniques were used to avoid disruptions
  - Disruption probability was reduced from 48% to 14% in high β_N/l_i plasmas with dual field component (radial and poloidal) active control
  - A model-based state space controller sustained long-pulse, high-β_N discharges with
- Dedicated resonant field amplification (RFA) experiments in NSTX revealed key dependencies of stability on plasma parameters
  - RFA measurements add additional support to the established theory of resistive wall mode (RWM) stability through kinetic mode-particle resonances
  - Stability is weakest at intermediate, not the highest, values of β_N/l_i, in agreement with other NSTX active control experiments
  - Relatively stable plasmas appear to benefit from reduced collisionality, in agreement with expectation from kinetic theory
- Application of the model to ITER plasmas indicates
  - Alpha particles may be needed for RWM stability
  - ITBs may be beneficial to RWM stability by lowering the E×B frequency

Supported by U.S. Department of Energy Contracts: DE-FG02-99ER54524, DE-AC02-09CH11466, and DE-FG02-93ER54215

Extra Slides

NSTX-U

Supported by

U.S. DEPARTMENT OF ENERGY | Office of Science

Global Mode Control and Stabilization for Disruption Avoidance in High-β NSTX Plasmas

J.W. Berkery[1], S.A. Sabbagh[1], A. Balbaky[1], R.E. Bell[2], R. Betti[3], J.M. Bialek[1], A. Diallo[2], D.A. Gates[2], S.P. Gerhardt[2], O.N. Katsuro-Hopkins[1], B.P. LeBlanc[2], J. Manickam[2], J.E. Menard[2], Y.S. Park[1], M. Podestà[2], F. Poli[2], H. Yuh[4]

[1]Columbia U., [2]PPPL, [3]U. Rochester, [4]Nova Photonics

Coll of Wm & Mary
Columbia U
CompX
General Atomics
FIU
INL
Johns Hopkins U
LANL
LLNL
Lodestar
MIT
Lehigh U
Nova Photonics
ORNL
PPPL
Princeton U
Purdue U
SNL
Think Tank, Inc.
UC Davis
UC Irvine
UCLA
UCSD
U Colorado
U Illinois
U Maryland
U Rochester
U Tennessee
U Tulsa
U Washington
U Wisconsin
X Science LLC

Culham Sci Ctr
York U
Chubu U
Fukui U
Hiroshima U
Hyogo U
Kyoto U
Kyushu U
Kyushu Tokai U
NIFS
Niigata U
U Tokyo
JAEA
Inst for Nucl Res, Kiev
Ioffe Inst
TRINITI
Chonbuk Natl U
NFRI
KAIST
POSTECH
Seoul Natl U
ASIPP
CIEMAT
FOM Inst DIFFER
ENEA, Frascati
CEA, Cadarache
IPP, Jülich
IPP, Garching
ASCR, Czech Rep

24th IAEA Fusion Energy Conference
San Diego, CA
October 8 – 13, 2012

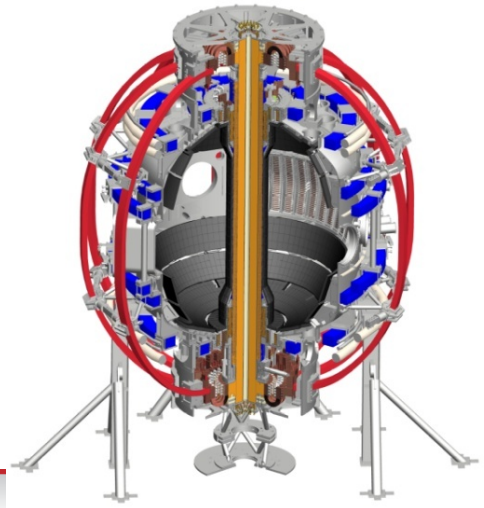

State derivative feedback algorithm used for current control

State equations to advance

$$\dot{\vec{x}} = A\vec{x} + B\vec{u} \qquad \vec{u} = -K_c\vec{x} = \dot{I}_{cc}$$

$$\vec{y} = C\vec{x} + D\vec{u}$$

Control vector, u; controller gain, K_c

Observer est., y; observer gain, K_o ; D = 0

K_c , K_o computed by standard methods (e.g. Kalman filter used for observer)

Advance discrete state vector

$$\hat{\vec{x}}_t = A\vec{x}_{t-1} + B\vec{u}_{t-1}; \hat{\vec{y}}_t = C\hat{\vec{x}}_t$$

"time update"

$$\vec{x}_{t+1} = \hat{\vec{x}}_t + A^{-1}K_o(\vec{y}_{sensors(t)} - \hat{\vec{y}}_t)$$

"measurement update"

State derivative feedback: superior control approach

$$\dot{\vec{x}} = A\vec{x} + B\vec{u} \qquad \vec{u} = -\hat{K}_c\dot{\vec{x}} \longrightarrow \vec{I}_{cc} = -\hat{K}_c\vec{x}$$

$$\dot{\vec{x}} = ((\mathrm{I} + B\hat{K}_c)^{-1}A)\vec{x}$$

new Ricatti equations to solve to derive control matrices – still "standard" solutions in control theory literature

[T.H.S. Abdelaziz, M. Valasek, Proc. of 16th IFAC World Congress (2005)]

Requests for an electronic copy

Supported by U.S. Department of Energy Contracts: DE-FG02-99ER54524, DE-AC02-09CH11466, and DE-FG02-93ER54215

Improving quantitative agreement consistently: EPs are stabilizing; Anisotropic distribution impacts stability

$$\delta W_K \sim \left[\frac{1}{\langle \omega_D \rangle + l\omega_b - i\nu_{\text{eff}} + \omega_E} \right]$$

small for Energetic Particles (EPs)

- EPs provide stabilizing force that is nearly independent of ω_ϕ
- EPs generally are not in mode resonance, so the effect is not energy dissipation, but rather a restoring force

[J.W. Berkery *et al.*, Phys. Plasmas **17**, 082504 (2010)]

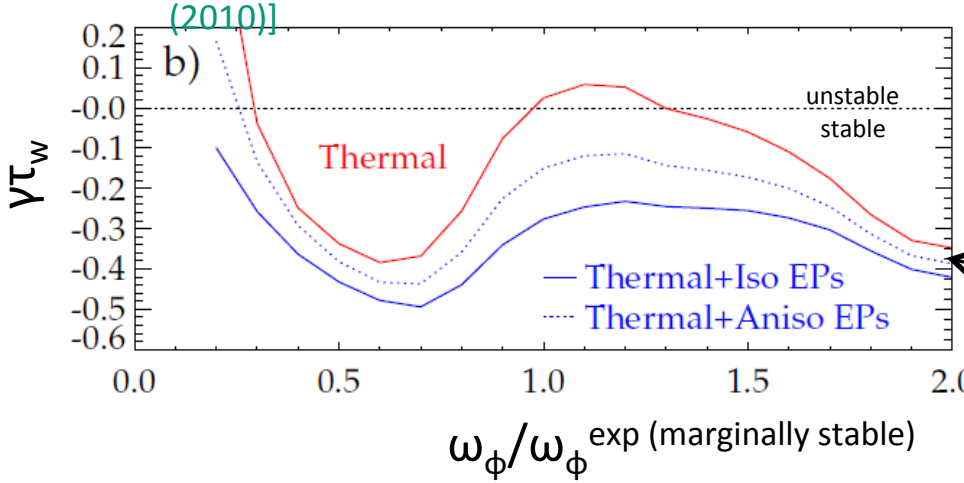

Beam ions are anisotropic

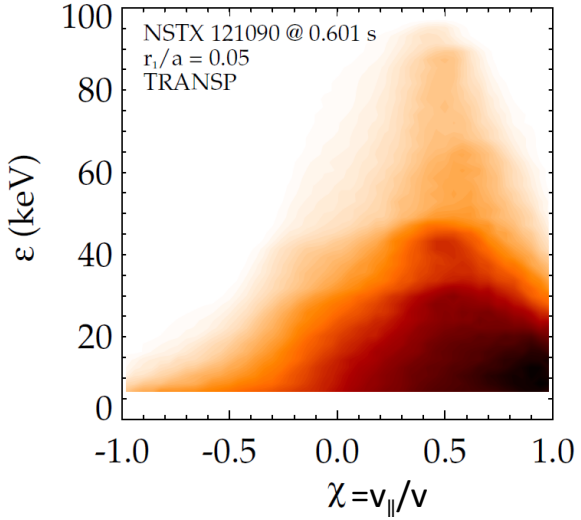

$$f(\varepsilon, \Psi, \chi) = \frac{C(\Psi)}{\varepsilon^{\frac{3}{2}} + \varepsilon_c^{\frac{3}{2}}} \frac{e^{-(\chi-\chi_0)^2/\delta\chi^2}}{\delta\chi}$$

Addition of simple anisotropy model ($\chi_0 = 0.75$, $\delta\chi = 0.25$) reduces stabilizing effect, consistent with quantitative comparison to NSTX plasmas

Pressure anisotropy leads to a modification of the Energy Principle

$$-i\omega\tau_w = -\frac{\delta W_V^\infty + \delta W_F + \delta W_A + \delta W_K}{\delta W_V^b + \delta W_F + \delta W_A + \delta W_K}$$

δW_V : usual changes in vacuum potential energy without a wall, and with an ideal wall

δW_F : usual isotropic fluid term

δW_A : anisotropic fluid correction

δW_K : kinetic term (also modified by anisotropy)

$$\omega = \omega_r + i\gamma$$

ω_r : real mode rotation frequency

γ : RWM growth rate

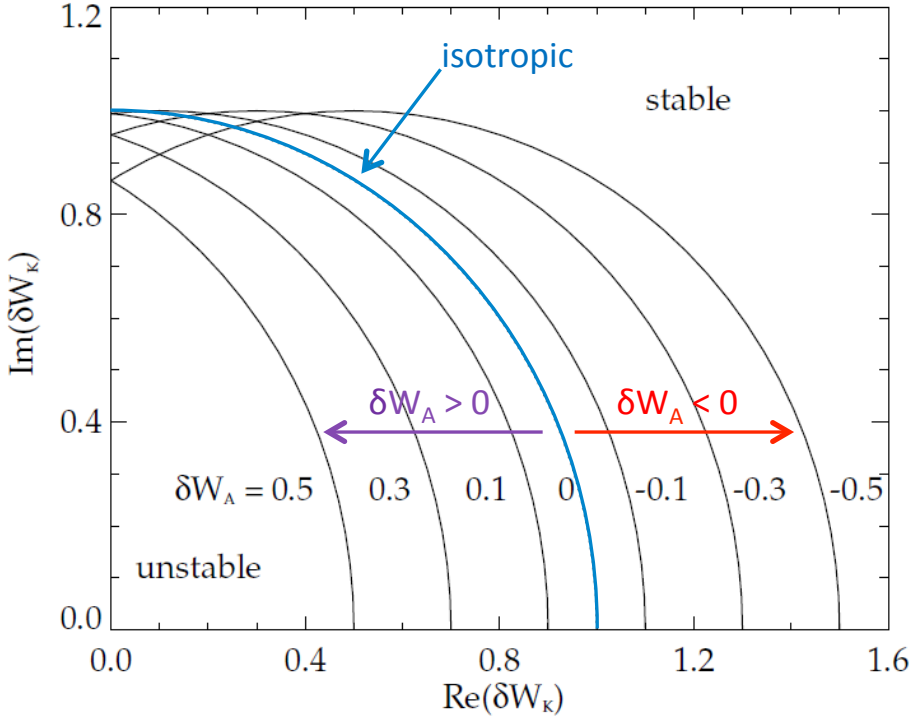

Stability diagram showing contours of $\gamma\tau_w = 0$ on $\mathrm{Re}(\delta W_K)$ vs. $\mathrm{Im}(\delta W_K)$ with $\delta W_\infty = -1$ and $\delta W_b = 1$ [arb.].

Positive δW_A shifts the unstable region to the left (destabilizing ballooning term reduced), negative δW_A to the right (ballooning term increased).

The kinetic approach is used to obtain δW_K; Anisotropic distribution functions affect the kinetic terms

δW terms are calculated starting from a plasma force balance:

$$\delta W = \frac{1}{2}\int \boldsymbol{\xi}_\perp^* \cdot \left[\mathbf{j_0}\times\tilde{\mathbf{B}} + \tilde{\mathbf{j}}\times\mathbf{B_0} - \boldsymbol{\nabla}\cdot\tilde{\mathbb{P}}\right] d\mathbf{V}$$

with: $$\mathbb{P} = p_{\|}\hat{\mathbf{b}}\hat{\mathbf{b}} + p_\perp\left(\hat{\mathbf{I}} - \hat{\mathbf{b}}\hat{\mathbf{b}}\right)$$

CGL pressures are akin to assumption of fast rotating mode (*not the RWM*), and will not be used. Instead in the kinetic approach, the perturbed pressures are calculated rigorously from the perturbed distribution function:

$$\tilde{f}_j = -\boldsymbol{\xi}_\perp\cdot\boldsymbol{\nabla}f_j + Z_j e\frac{\partial f_j}{\partial\varepsilon}\tilde{\boldsymbol{\Phi}} + im_j\left(\omega\frac{\partial f_j}{\partial\varepsilon} - n\frac{\partial f_j}{\partial P_\phi}\right)(\mathbf{v}\cdot\boldsymbol{\xi}_\perp - \tilde{s}_j) - \frac{m_j}{B}\frac{\partial f_j}{\partial\mu}\left(-i\omega\boldsymbol{\xi}_\perp\cdot\mathbf{v}_\perp + \frac{\mu}{m_j}\tilde{\mathbf{B}}_{\|} + \frac{v_{\|}}{B}\mathbf{v}_\perp\cdot\tilde{\mathbf{B}}\right)$$

Kinetic effects are modified by inclusion of bi-Maxwellian or anisotropic slowing-down distributions in frequency resonance fraction calculation

$$\delta W_K = \sum_j\sum_{l=-\infty}^{\infty} 2\sqrt{2}\pi^2\int\int\int\left[|\langle H/\hat{\varepsilon}\rangle|^2\frac{(\omega - n\omega_E)\frac{\partial f_j}{\partial\varepsilon} - \frac{n}{Z_j e}\frac{\partial f_j}{\partial\Psi}}{n\langle\omega_D^j\rangle + l\omega_b^j - i\nu_{\text{eff}}^j + n\omega_E - \omega}\right]\frac{\hat{\tau}}{m_j^{\frac{3}{2}}B}|\chi|\hat{\varepsilon}^{\frac{5}{2}}d\hat{\varepsilon}d\chi d\boldsymbol{\Psi},$$

Additionally, an anisotropic correction to the fluid term principally modifies the ballooning destabilization term

$$\delta W_F = \frac{1}{2}\int\left\{\underbrace{\left(\underbrace{-\frac{|\tilde{\boldsymbol{B}}_\perp|^2}{\mu_0}}_{\text{shear Alfvén}} \underbrace{-\frac{B^2}{\mu_0}|\boldsymbol{\nabla}\cdot\boldsymbol{\xi}_\perp + 2\boldsymbol{\xi}_\perp\cdot\boldsymbol{\kappa}|^2}_{\text{fast magneto-acoustic}} \underbrace{+ j_\parallel\left(\boldsymbol{\xi}_\perp^*\times\hat{\boldsymbol{b}}\right)\cdot\tilde{\boldsymbol{B}}_\perp}_{\text{kink}}\right)}_{3} \underbrace{+2\left(\boldsymbol{\kappa}\cdot\boldsymbol{\xi}_\perp^*\right)\left(\boldsymbol{\xi}_\perp\cdot\boldsymbol{\nabla}p_{\text{avg}}\right)}_{\text{ballooning}}\right\} d\mathbf{V},$$

$$\delta W_A = \frac{1}{2}\int\left\{\underbrace{(\sigma-1)\left(-\frac{|\tilde{\boldsymbol{B}}_\perp|^2}{\mu_0} - \frac{B^2}{\mu_0}|\boldsymbol{\nabla}\cdot\boldsymbol{\xi}_\perp + 2\boldsymbol{\xi}_\perp\cdot\boldsymbol{\kappa}|^2 + j_\parallel\left(\boldsymbol{\xi}_\perp^*\times\hat{\boldsymbol{b}}\right)\cdot\tilde{\boldsymbol{B}}_\perp\right)}_{3} - 2B\left|\boldsymbol{\nabla}\cdot\boldsymbol{\xi}_\perp + \boldsymbol{\kappa}\cdot\boldsymbol{\xi}_\perp\right|^2\frac{\partial p_{\text{avg}}}{\partial B}\right\} d\mathbf{V}$$

These will be small due to σ ≈ 1.

Note: terms 1, 2, and 3 together can be shown to be self-adjoint, so that $\delta W_F + \delta W_A$ is self-adjoint

4 ⟶ $$\delta W_{A2} = \sqrt{2}\pi^2\int\int\int\frac{1}{m_j^{\frac{3}{2}}}\left|\boldsymbol{\nabla}\cdot\boldsymbol{\xi}_\perp + \boldsymbol{\kappa}\cdot\boldsymbol{\xi}_\perp\right|^2\left(\chi^4-1\right)\frac{\partial f_j}{\partial\chi}\frac{\hat{\tau}}{B}\varepsilon^{\frac{3}{2}}d\varepsilon d\chi d\boldsymbol{\Psi}.$$

The anisotropic correction to the ballooning term depends upon the derivative of the distribution function with respect to pitch angle, $\chi = v_\parallel/v$.

Two anisotropic distributions are considered: bi-Maxwellian for thermal particles, slowing-down for energetic particles

A bi-Maxwellian distribution with different temperatures ⊥ and ∥ to the magnetic field:

$$f_j^{bM}(\varepsilon,\Psi,\chi) = n_j \left(\frac{m_j}{2\pi}\right)^{\frac{3}{2}} \frac{1}{T_{j\perp} T_{j\parallel}^{\frac{1}{2}}} e^{-\varepsilon\chi^2/T_{j\parallel}} e^{-\varepsilon(1-\chi^2)/T_{j\perp}}$$

A slowing down distribution function with a Gaussian distribution of particles in χ:

$$f_j^b(\varepsilon,\Psi,\chi) = n_j A_b \left(\frac{m_j}{\varepsilon_b}\right)^{\frac{3}{2}} \frac{1}{\hat{\varepsilon}^{\frac{3}{2}} + \hat{\varepsilon}_c^{\frac{3}{2}}} \frac{1}{\delta\chi} \left(\exp\left[\frac{-(\chi-\chi_0)^2}{\delta\chi^2}\right] + \exp\left[\frac{-(\chi+2+\chi_0)^2}{\delta\chi^2}\right] + \exp\left[\frac{-(\chi-2+\chi_0)^2}{\delta\chi^2}\right] \right)$$

Beam ions are injected with injection pitch angle χ_0 and initial spread $\delta\chi_0$

$f(\varepsilon,\chi)$ at a particular Ψ for an NSTX equilibrium from

a) TRANSP

b) model (with $\chi_0 = 0.5$ $\delta\chi_0 = 0.2$)

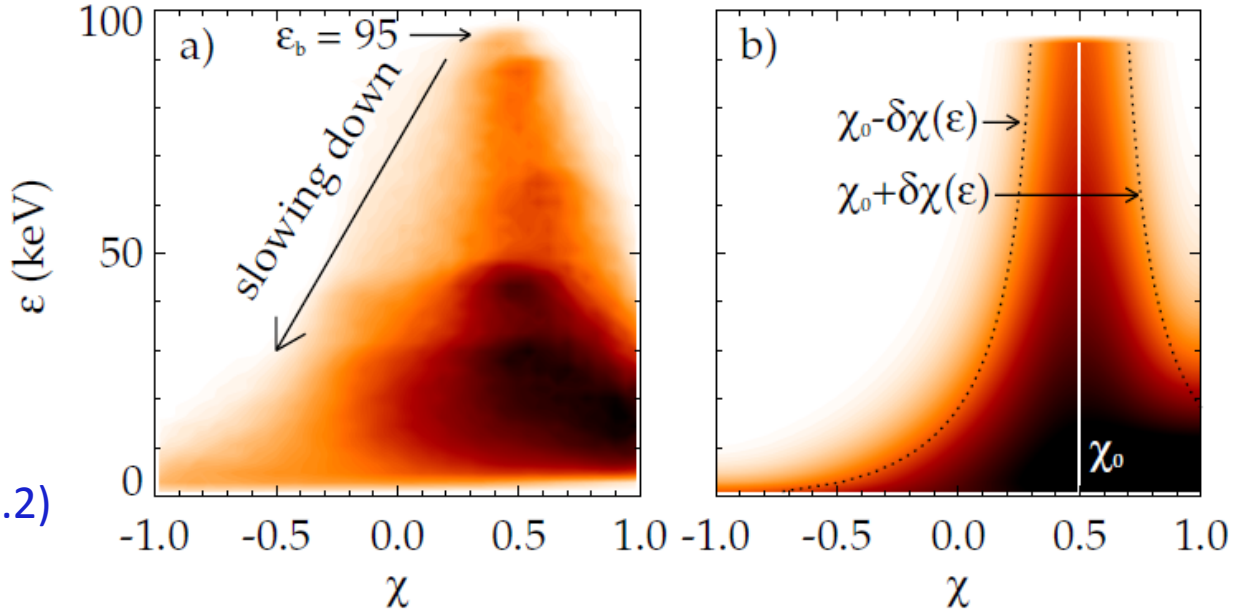

Anisotropy of thermal particles was explored through $T_{||}/T_{\perp}$; could potentially make an impact on the calculated RWM growth rate

Corrections to each fluid term

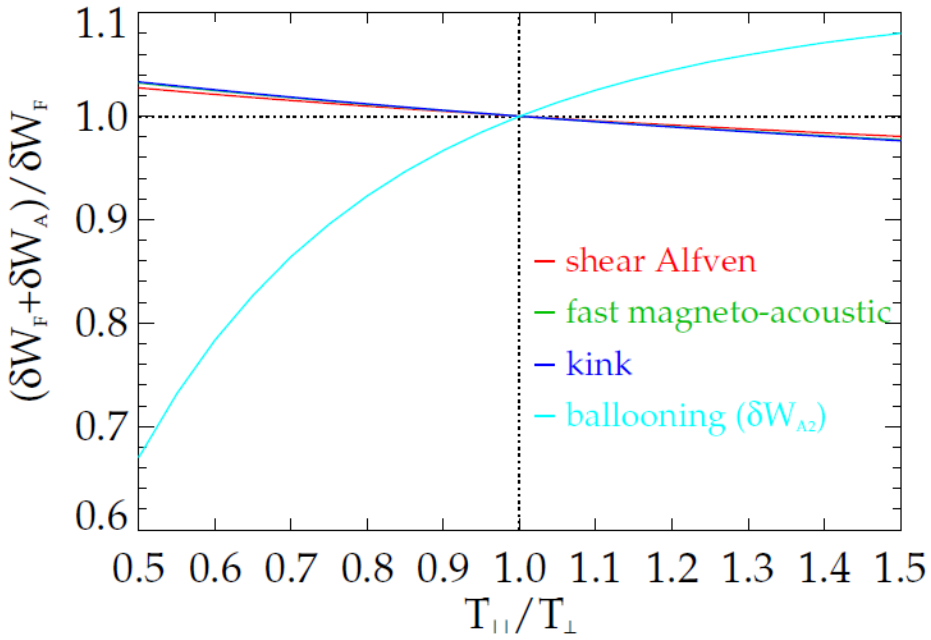

Impact of fluid corrections, and anisotropic kinetic effects on growth rate

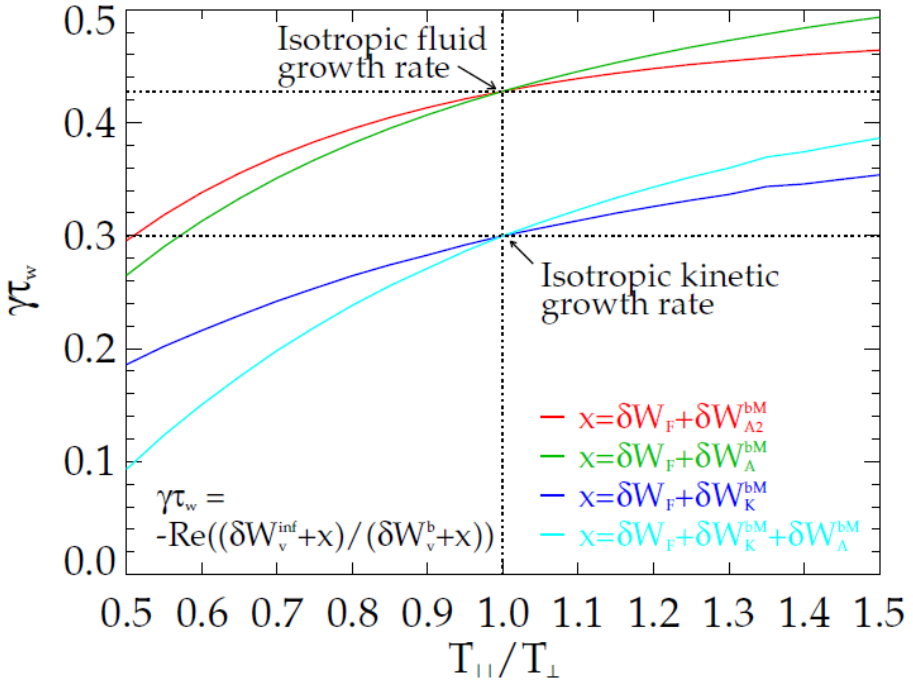

Simple Solov'ev test case used to explore the effects.

As $T_{||}/T_{\perp}$ is reduced, the destabilizing ballooning term is reduced.

As $T_{||}/T_{\perp}$ is reduced, the stabilizing kinetic term is increased.

Most applicable to experimental scenarios with RF heating (ITER).

Reduction in RWM fluid growth rate and reduction in RWM kinetic growth rate with both kinetic effects and fluid corrections.

Internal transport barriers may be beneficial to RWM stability by lowering the E×B frequency

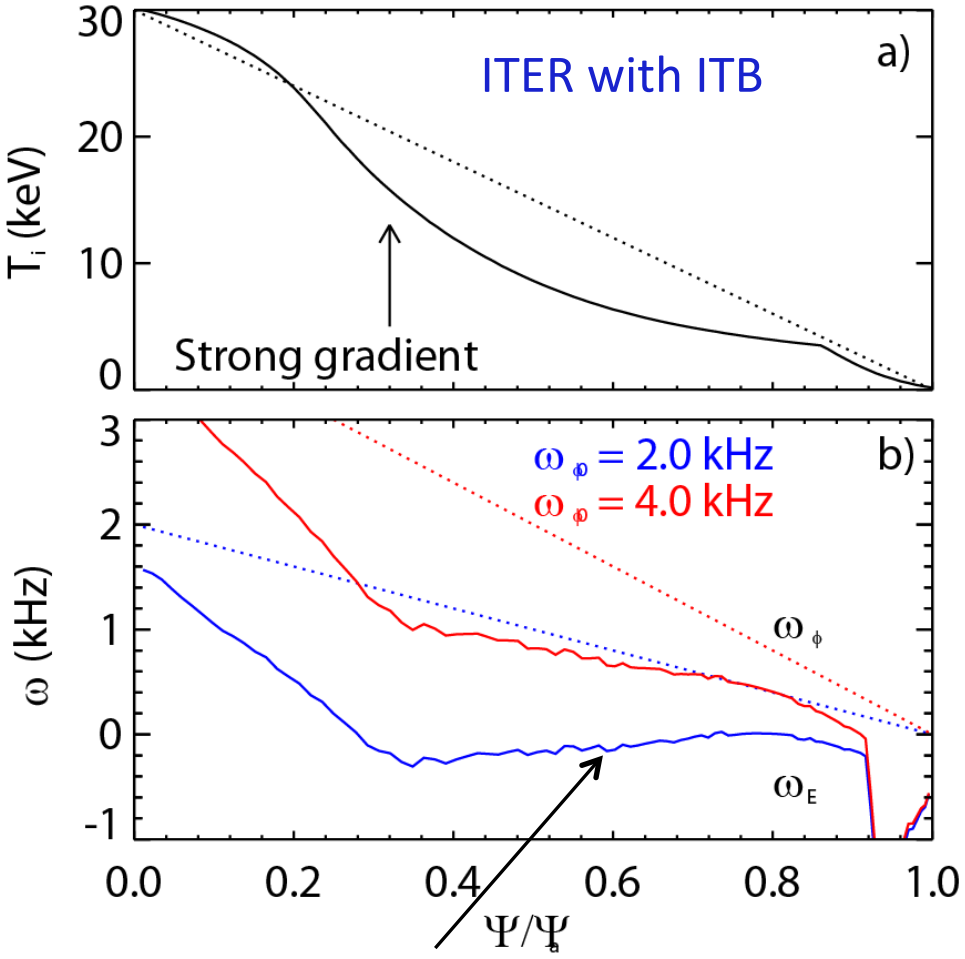

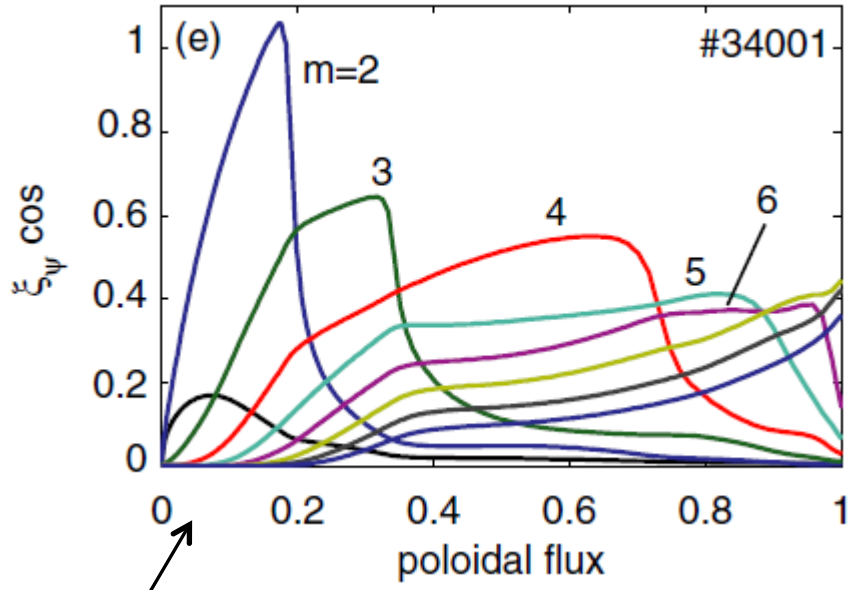

MISK Calculation

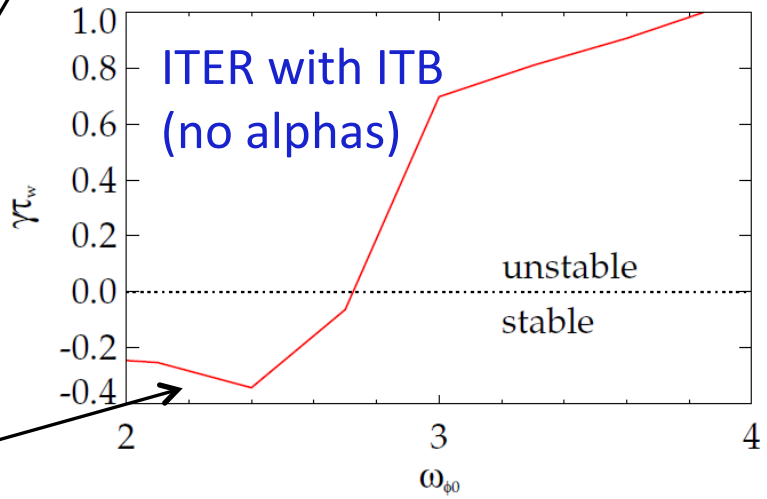

ITB lowers ω_E to ~0,
combined with "infernal" type eigenfunction:
predicted stability at low rotation without alphas

The RWM is identified in NSTX by a variety of observations

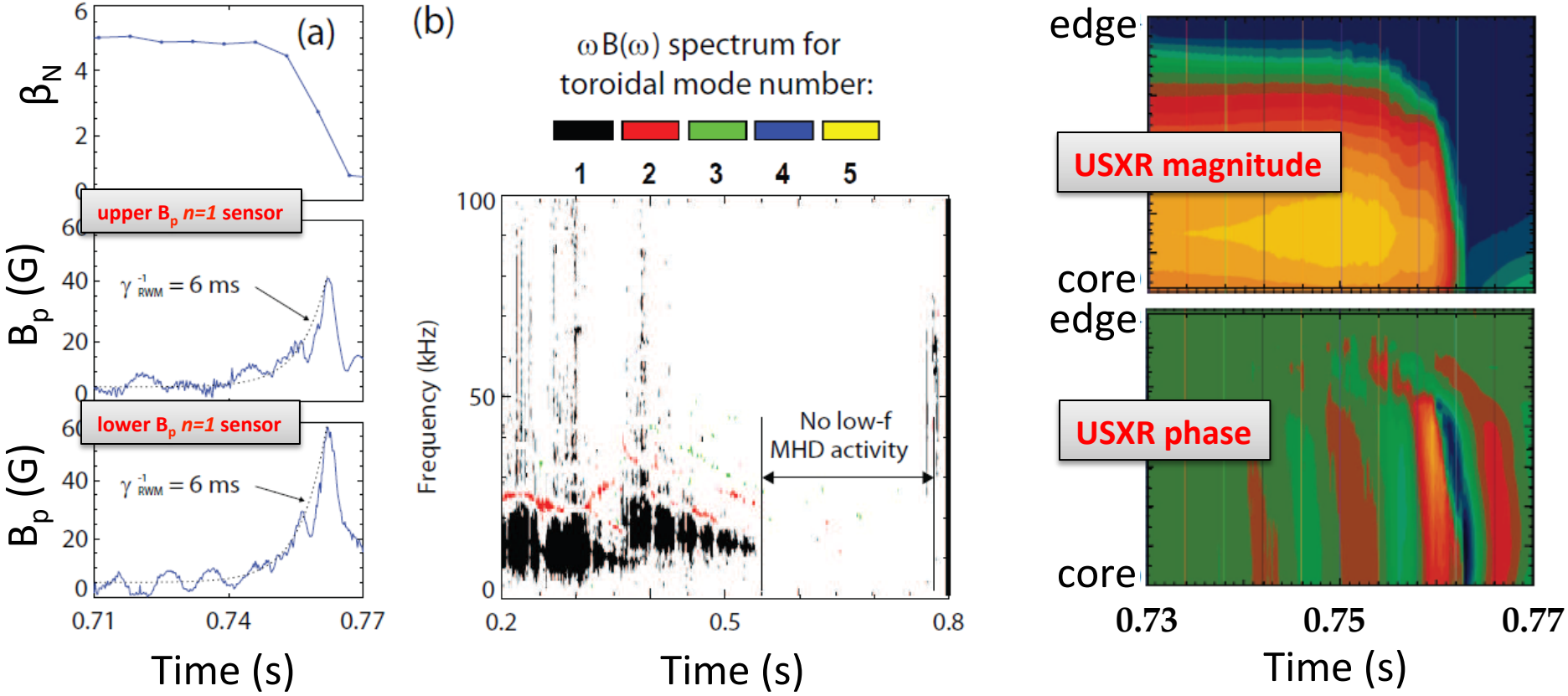

- Growing signal on low frequency poloidal magnetic sensors
- Global collapse in USXR signals, with no clear phase inversion
- Causes a collapse in β and disruption of the plasma

Future ST fusion applications will have high elongation, broad current profiles, high normalized beta

FNSF / ST-CTF

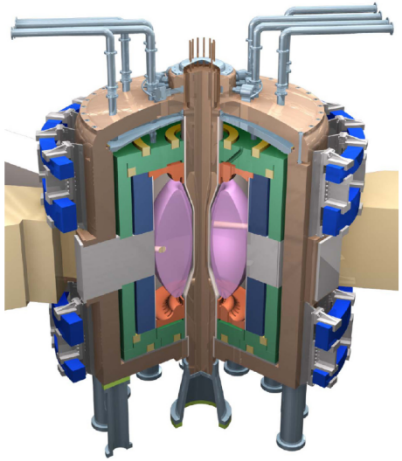

Y.K.M. Peng, et al., PPCF 47 (2005) B263

ST-Pilot (Q_{eng} = 1)

J. Menard, et al., IAEA FEC 2010 Paper FTP/2-2

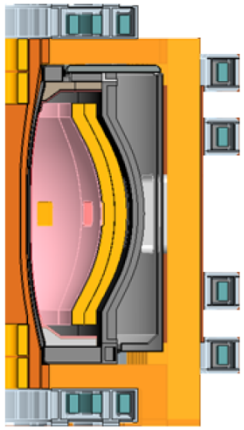

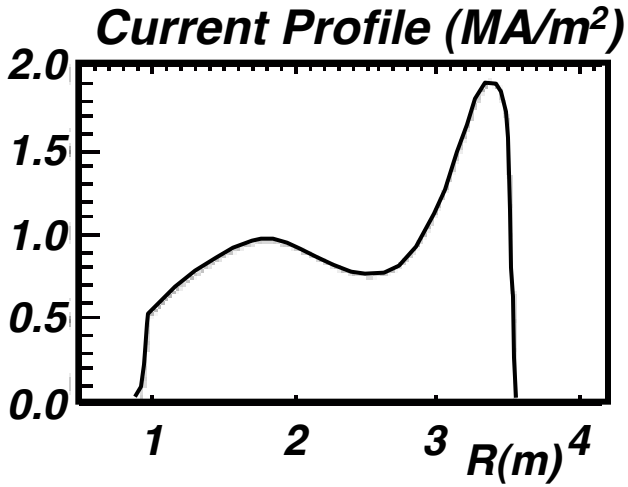

- Broad current profile → low $l_i = \langle B_p^2 \rangle / \langle B_p \rangle_\psi^2$, has global mode stability implications
  - Improved vertical (n = 0) and wall-stabilized, rotating kink (n =1) stability
  - Decreased RWM stability, influenced by ω_ϕ
  - "Troyon limit" (ideal, static n = 1 no-wall stability limit)

l_i = 0.47, κ = 3.2
R = 2.23 m, A = 1.7
I_p = 16 MA, B_t = 2.4T
β_N = 5.2, β_t = 30%

$\beta_N = 10^8 \beta_t a B_t / I_p$ = constant ~ 3; variants: $\beta_N \propto l_i$, $\beta_N \propto$ 1/(pressure peaking)

Operation at higher β_N possible by passive or active RWM stabilization ($\beta_t = 2\mu_0 \langle p \rangle / B_t^2$)